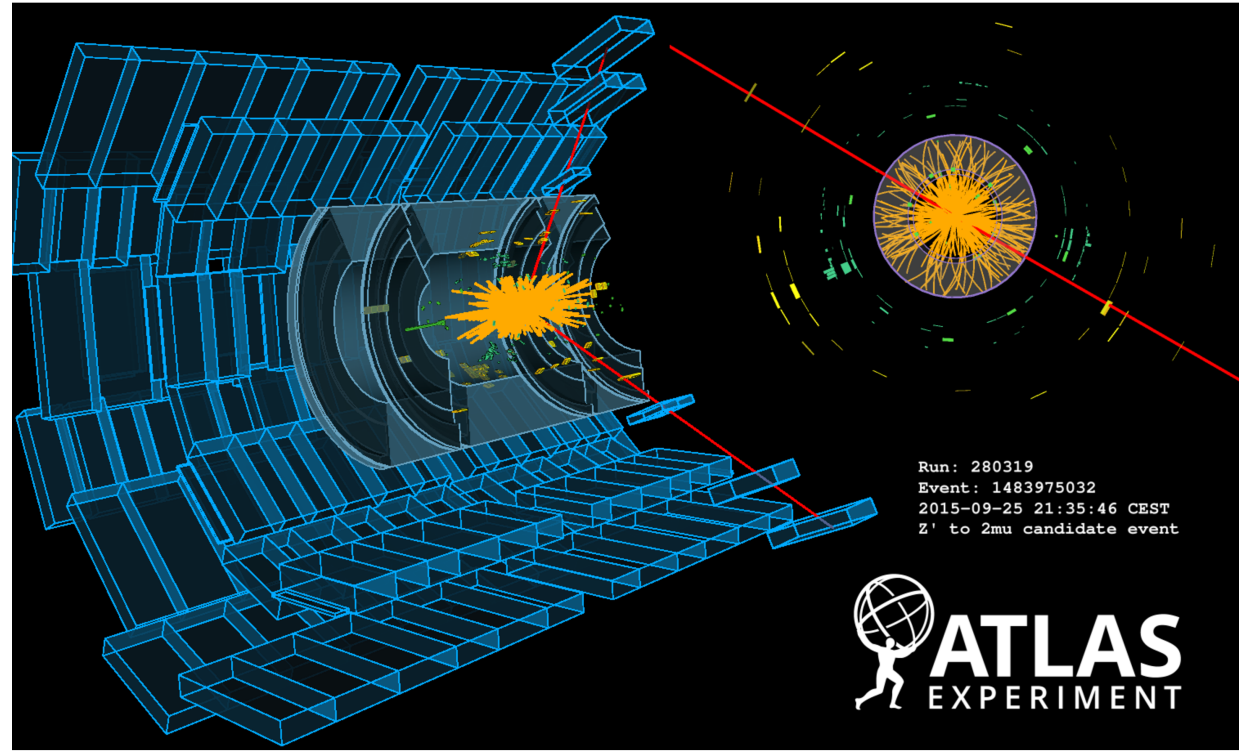
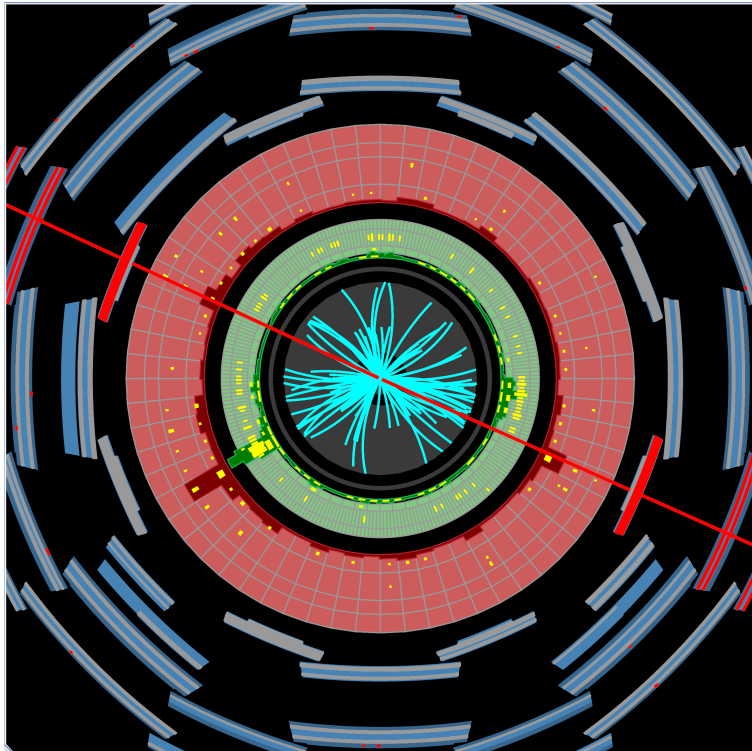


Search for the Z' Boson



Ph.D. Thesis Defense
East Lansing, Michigan, 25 Apr. 2018

Christopher Willis on behalf of the
ATLAS Collaboration

MICHIGAN STATE
UNIVERSITY



Introduction

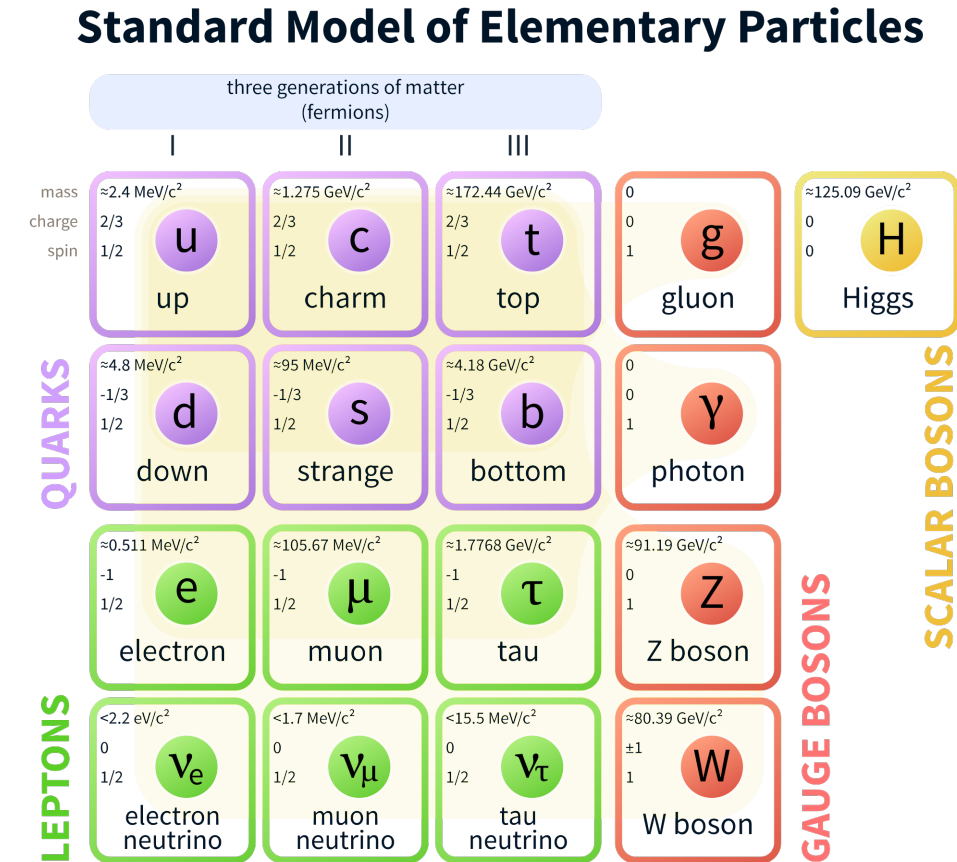
Part 1: Search for New Physics

Part 2: Reduction of PDF Uncertainty

Part I: Search for New Physics

Overview of the Standard Model

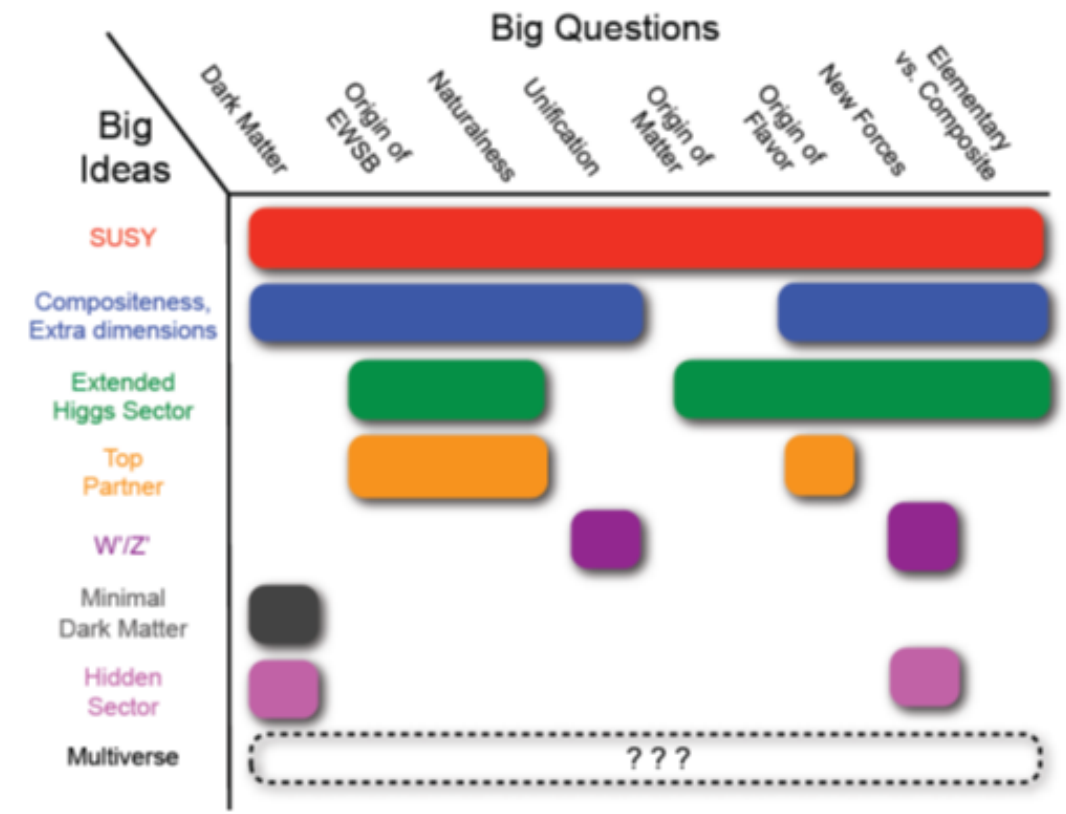
- Standard Model (SM) is relativistic quantum field theory (QFT)
- Explains fundamental interactions via local $SU(3)_C \times SU(2)_L \times U(1)_Y$ symmetry group
- Gauge symmetries give rise to strong, weak, electromagnetic interactions
- Extremely successful, well-tested theory



Limitations of the SM

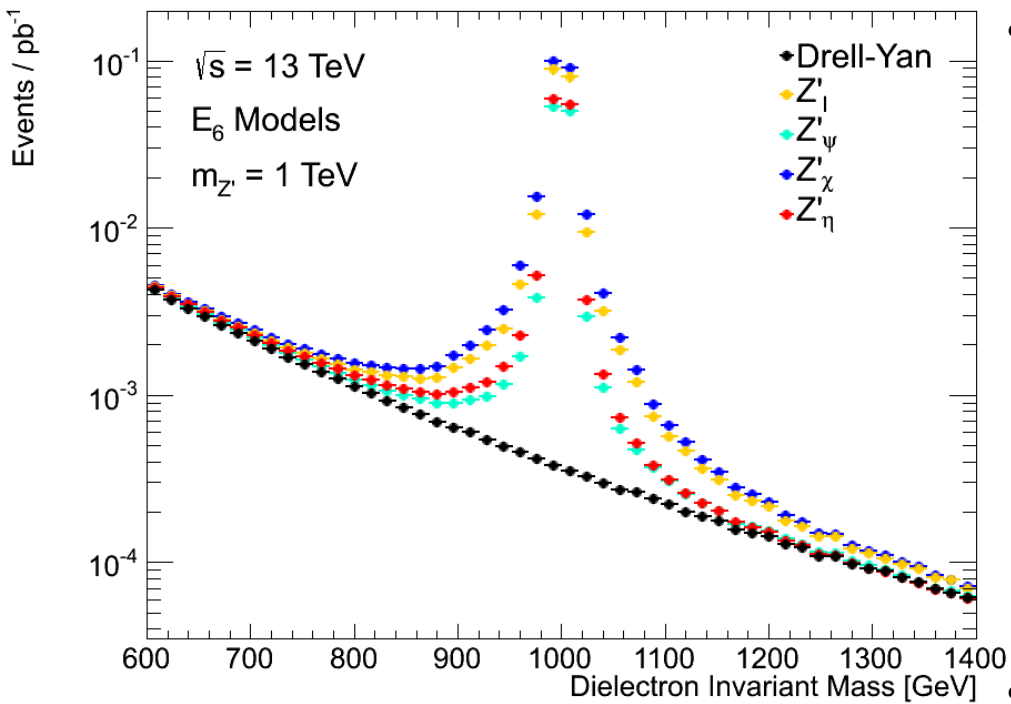
→ Despite its success, the Standard Model is almost certainty an incomplete theory!

- Phenomena not Explained
 - Dark Matter
 - Origin of neutrino masses
 - Baryon Asymmetry
 - Gravity and Dark Energy
- Conceptual Issues
 - Origin of Flavor
 - Number of free parameters
 - Hierarchy Problem
 - Unification of forces



Models with Extended Gauge Symmetries

→ Predict additional spin-1 gauge bosons (Z' , W')



- Motivated by Grand Unified Theories (GUTs), such as the **E₆ model**:
$$E_6 \rightarrow SO(10) \times U(1)_\psi \rightarrow SU(5) \times U(1)_\chi \times U(1)_\psi$$

GUT Decomposition SM Forces New Physics

 - $Z'(\theta_{E_6}) = Z'_\psi \cos \theta_{E_6} + Z'_\chi \sin \theta_{E_6}$
 - Different motivated values of angle θ lead to observable Z' states:
 $Z'_\psi, Z'_N, Z'_\eta, Z'_I, Z'_S$ and Z'_χ
- Motivated by **SSM**, simple extension of Standard Model
 - Z'_{SSM} assigned same fermion couplings as SM Z Boson

Large Hadron Collider: Facts and Figures

- Center-of-Mass Energy of $\sqrt{s} = 13 \text{ TeV}$
- Instantaneous Luminosity of $L = 10^{34} \text{ cm}^2 \text{ s}^{-1}$



Large Hadron Collider: Facts and Figures

- Center-of-Mass Energy of $\sqrt{s} = 13 \text{ TeV}$
- Instantaneous Luminosity of $L = 10^{34} \text{ cm}^2 \text{ s}^{-1}$



Number of expected events in LHC dataset

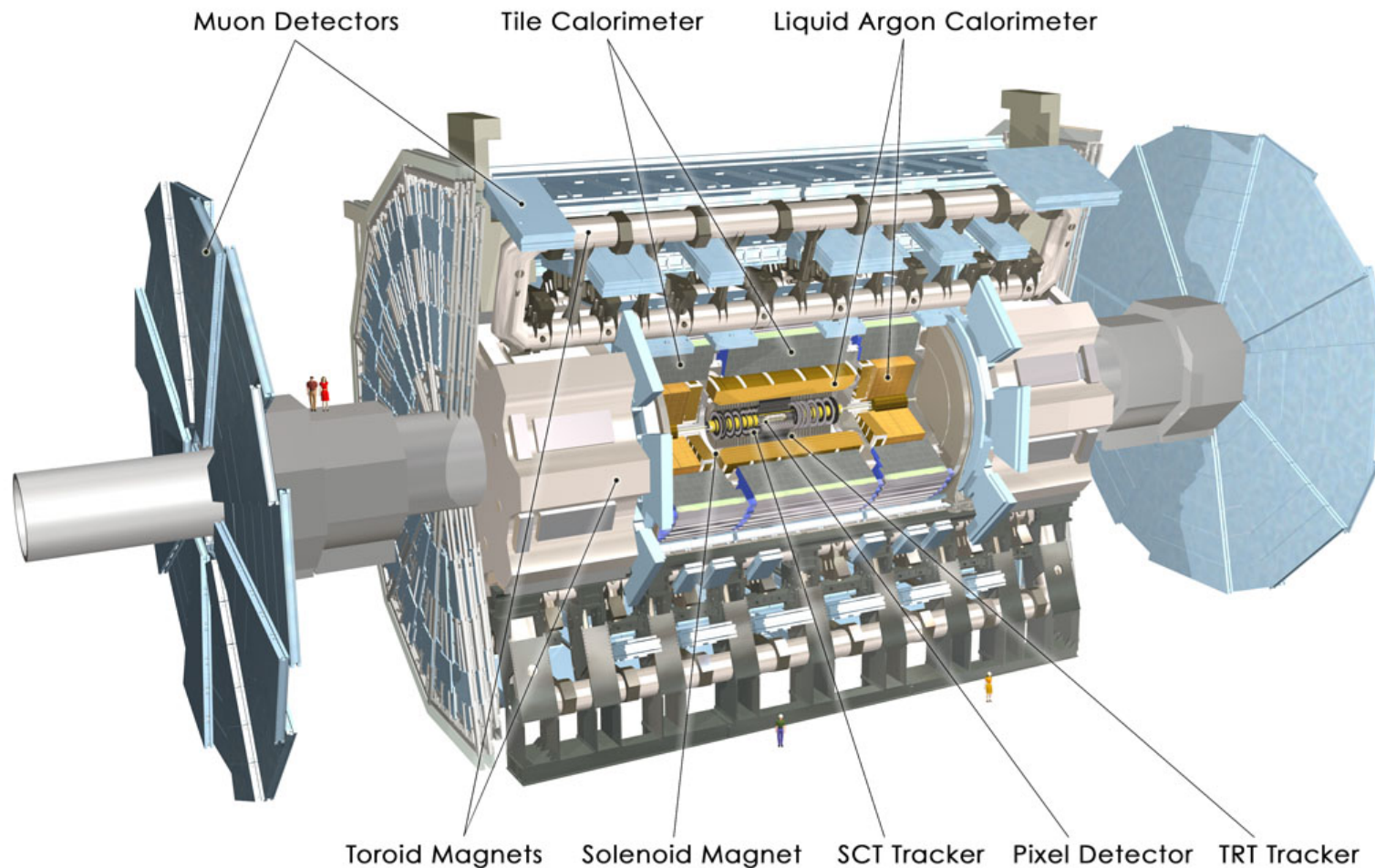
Integrated Luminosity of LHC dataset

$$N_{\text{evt}} = \sigma L_{\text{int}} = \sigma \int L \, dt$$

Scattering cross section for process of interest (e.g Z' production)

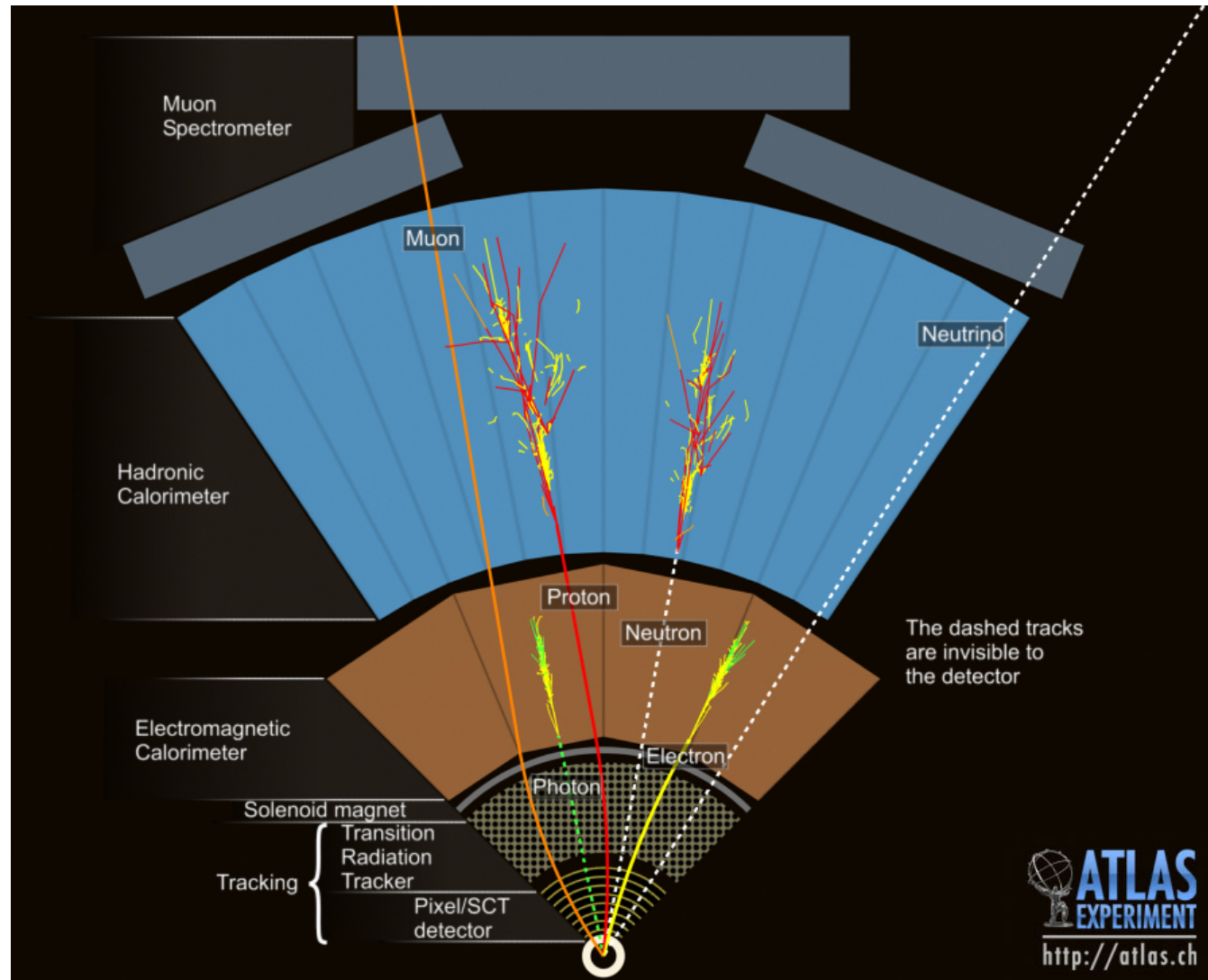
Overview of the ATLAS Detector

→ General purpose detector, designed with new physics in mind



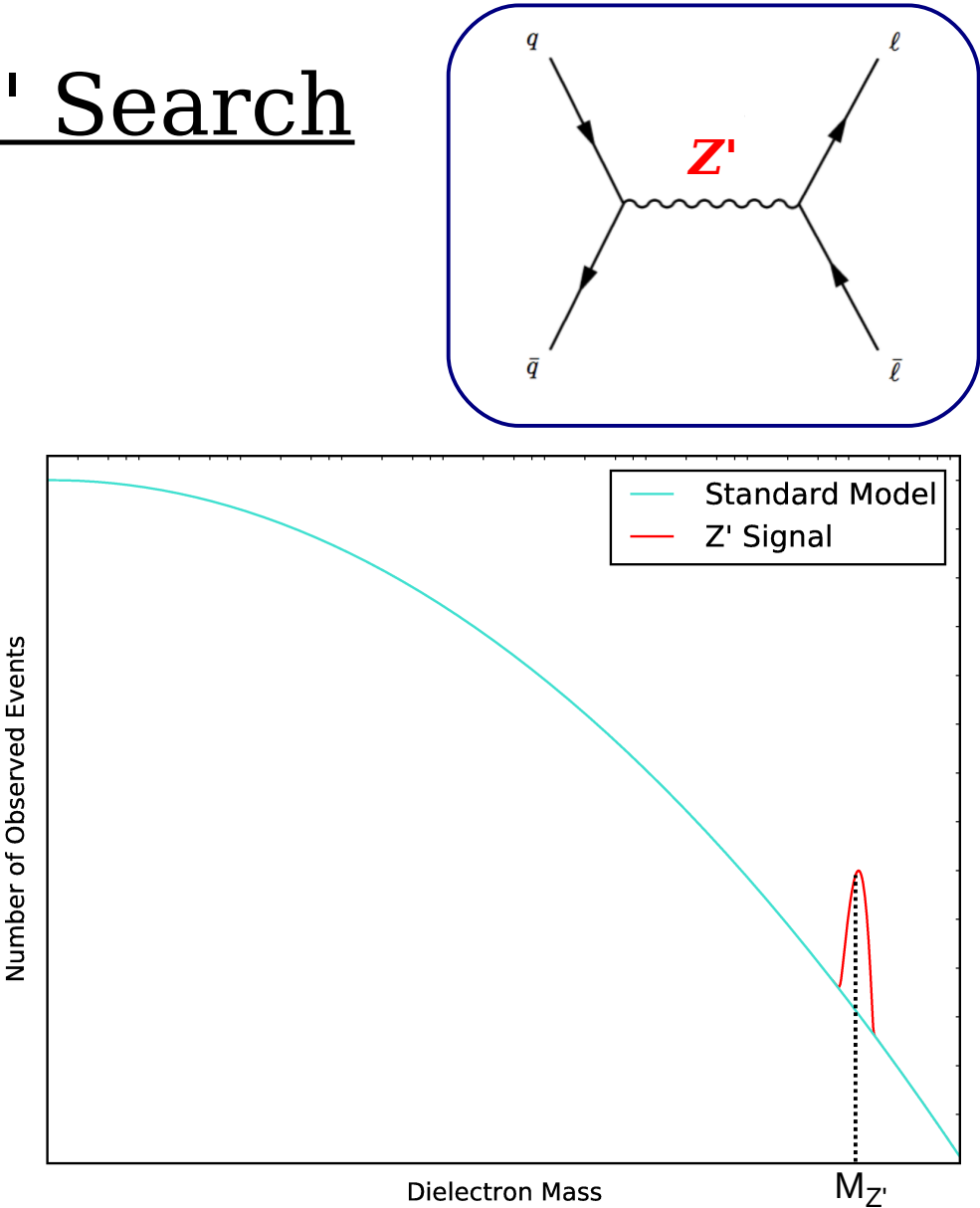
Particle Detection in ATLAS

- ATLAS can detect electrons, photons, jets, hadrons, muons, taus, and neutrinos
- Allows LHC pp events to be fully reconstructed



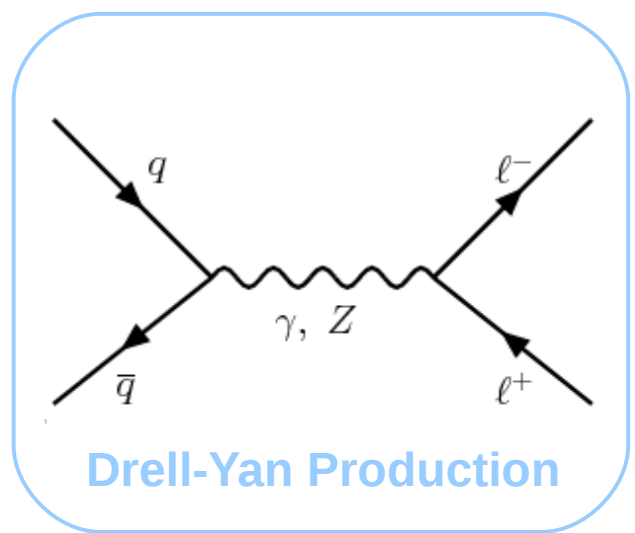
Analysis Strategy for Z' Search

- Want to identify $Z' \rightarrow e^+e^-$ decays in LHC pp collisions
- Perform classic “bump-hunt”
 - Select events with two good quality, high E_T electron candidates
 - Reconstruct the dielectron pair invariant mass
 - Perform a search for possible deviations from SM prediction
 - Set exclusion limits if no significant deviations found

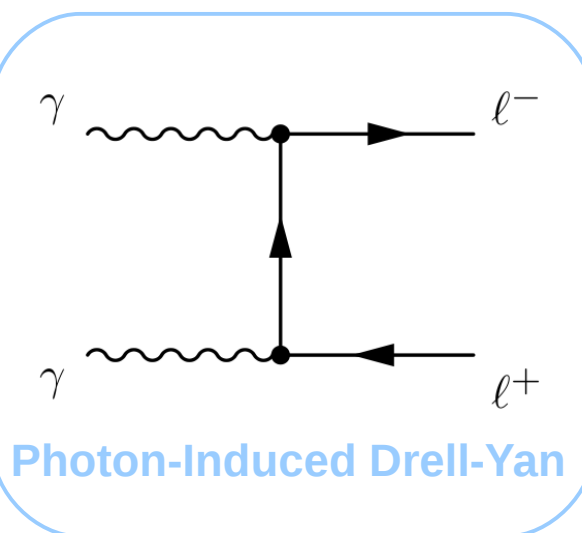


Data and Background Samples

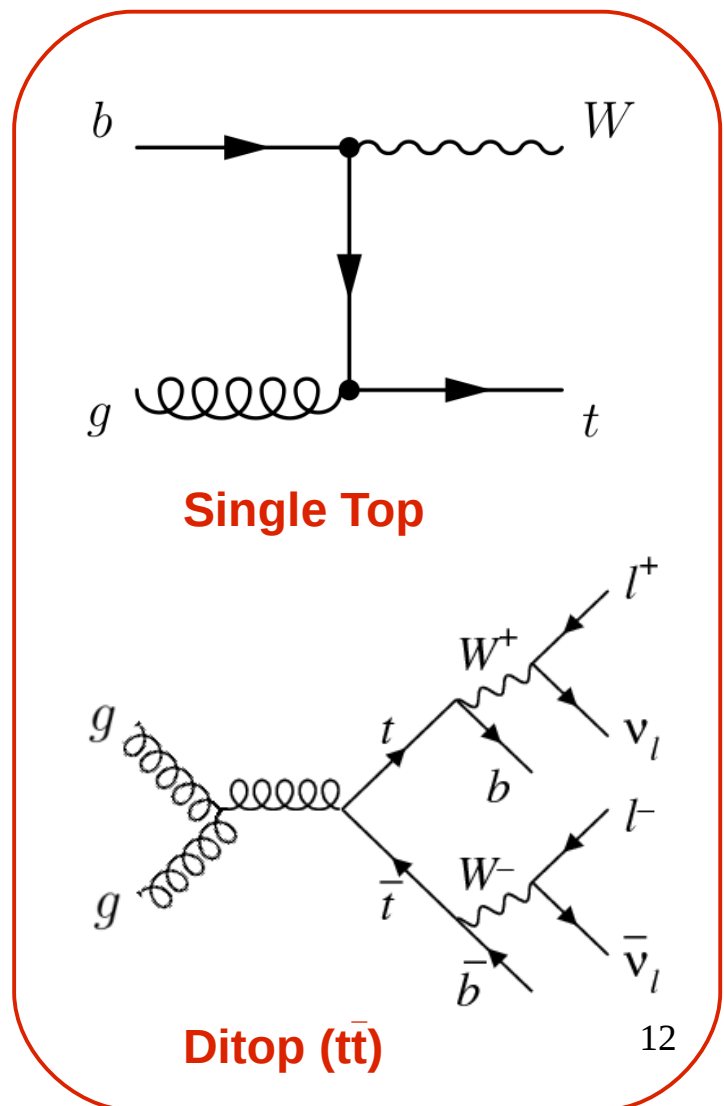
- Use full 2015+2016 ATLAS dataset (36.1/fb)
- Additional background processes result in dielectron final-states at the LHC
- Accounted for with monte-carlo simulation samples



Drell-Yan Production

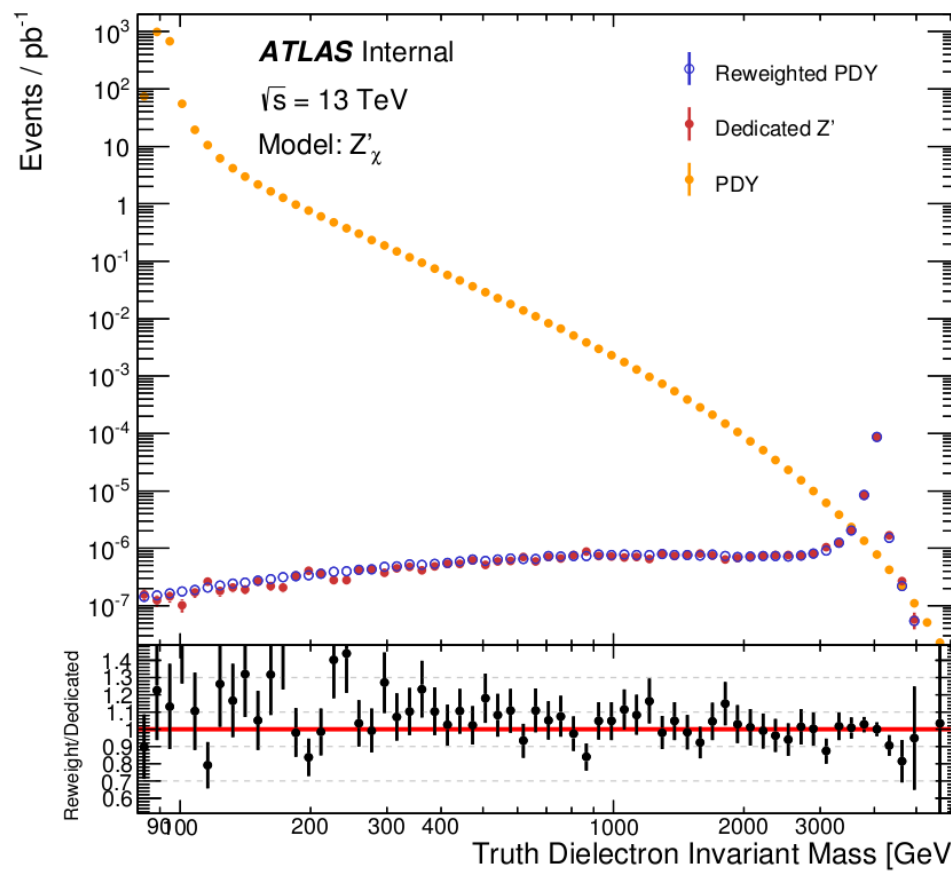


Photon-Induced Drell-Yan



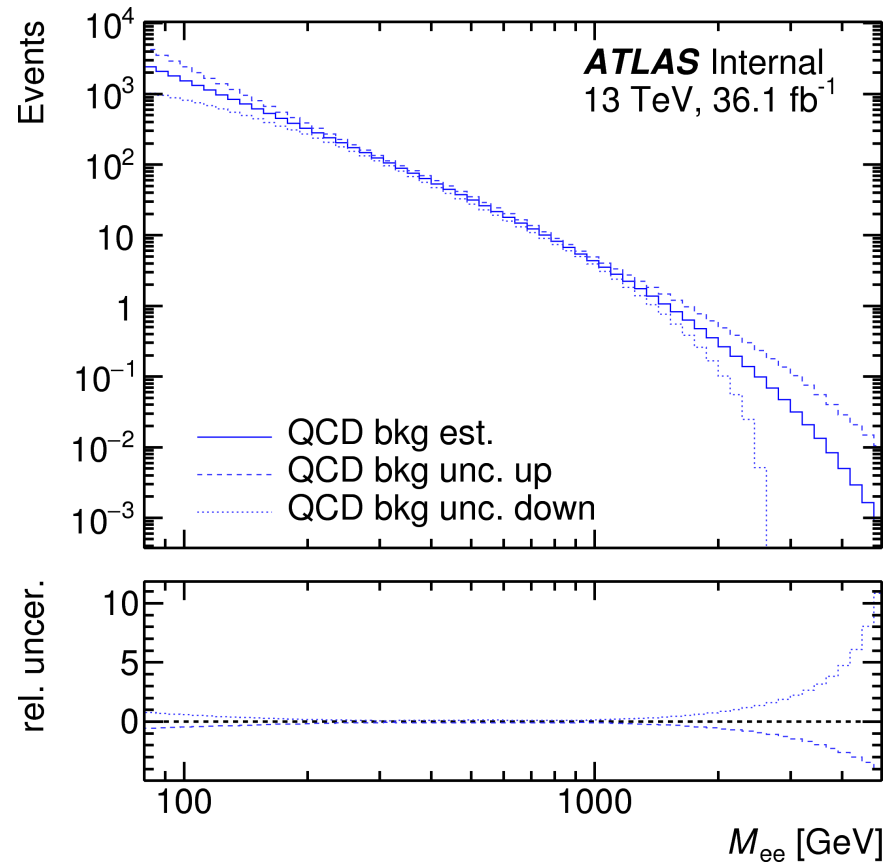
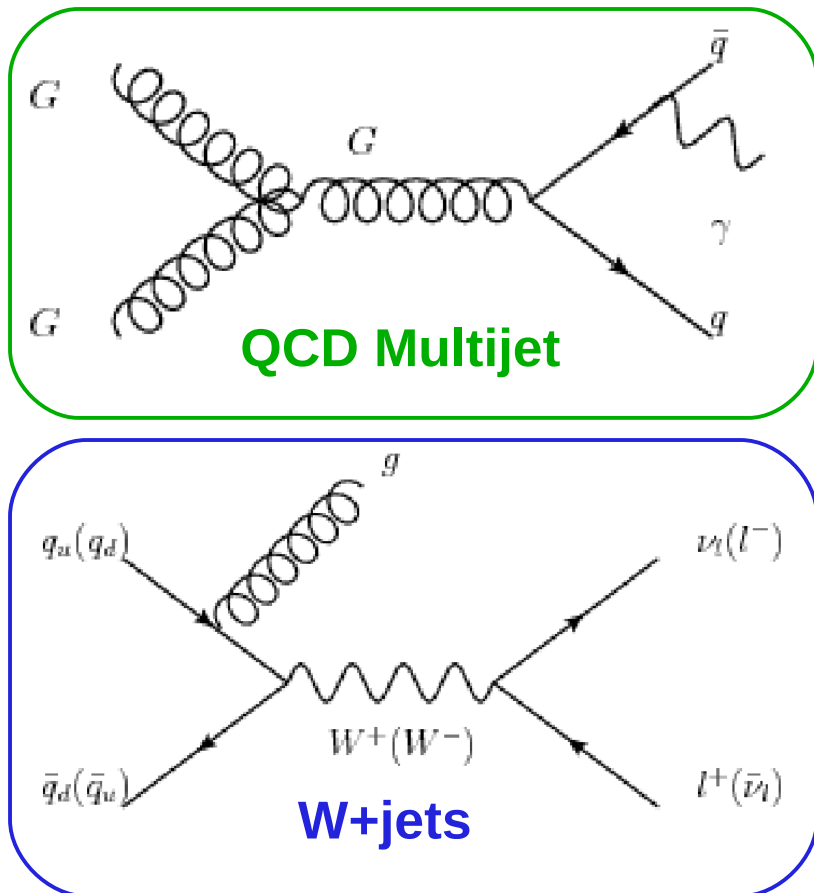
Signal Samples

- Signal Reweighting technique used to produce Z' signal samples
- Validated against small set of dedicated Z' signal MC
- Huge! No need for generation of additional dedicated MC samples



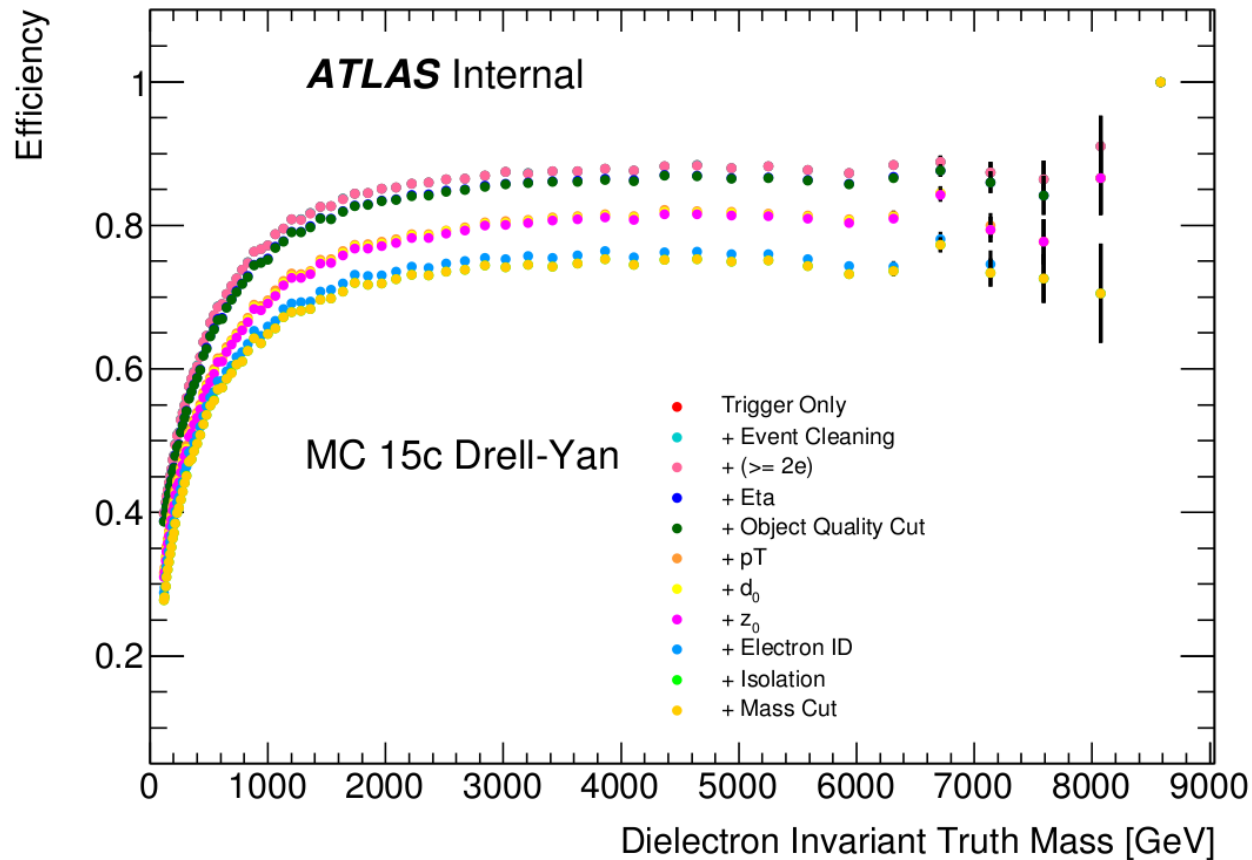
Fake Background Estimation

- Need to also account for the “fake” electron background
 - Events with **two jets** or **electron+jet** can pass signal selection if jet(s) mis-reconstructed as electron(s)
 - Background estimated using data-driven “Matrix Method” technique



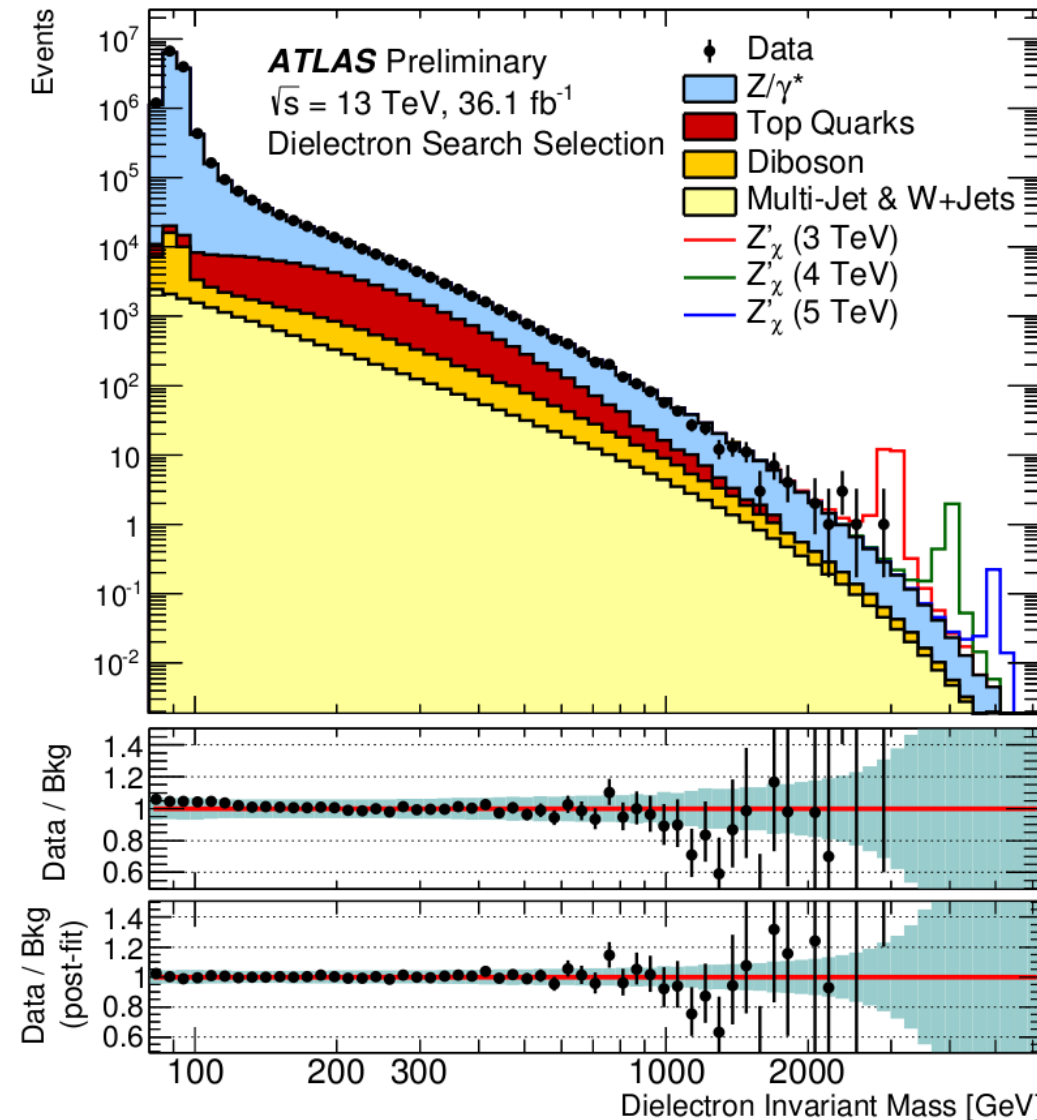
Employ Dielectron Event Selection

→ Select events with at least two high E_T , well isolated, well reconstructed electron candidates



→ Event Selection maximally efficient at high-mass, total efficiency $\sim 70\%$

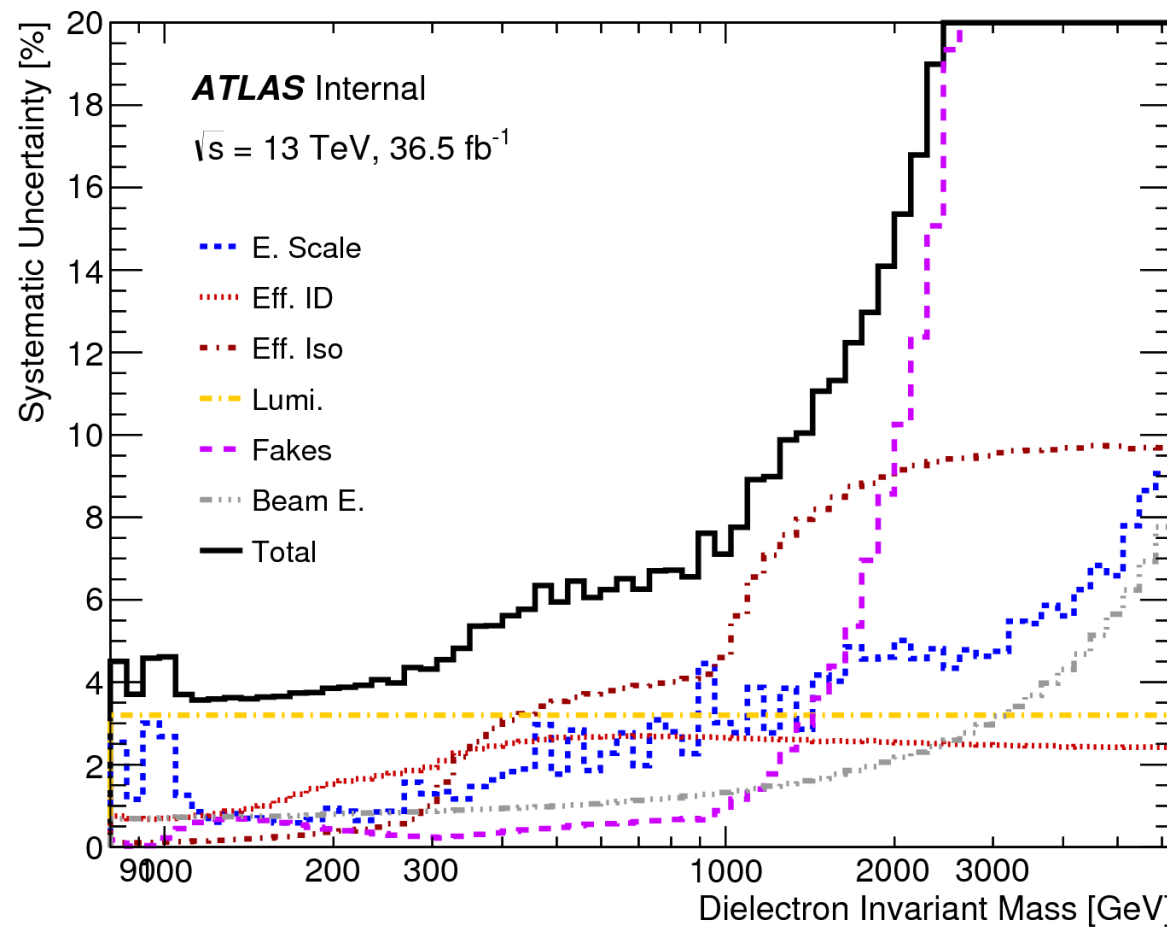
Comparing Data to Simulation Post-Selection



- Event Selection applied to data/MC
- Simulation scaled to 36.1/fb, stacked, and various corrections applied
- Several characteristic Z' signals overlaid
- Data agrees well with SM expectation
- Highest mass event at 2.9 TeV
- No obvious signal-like excess present

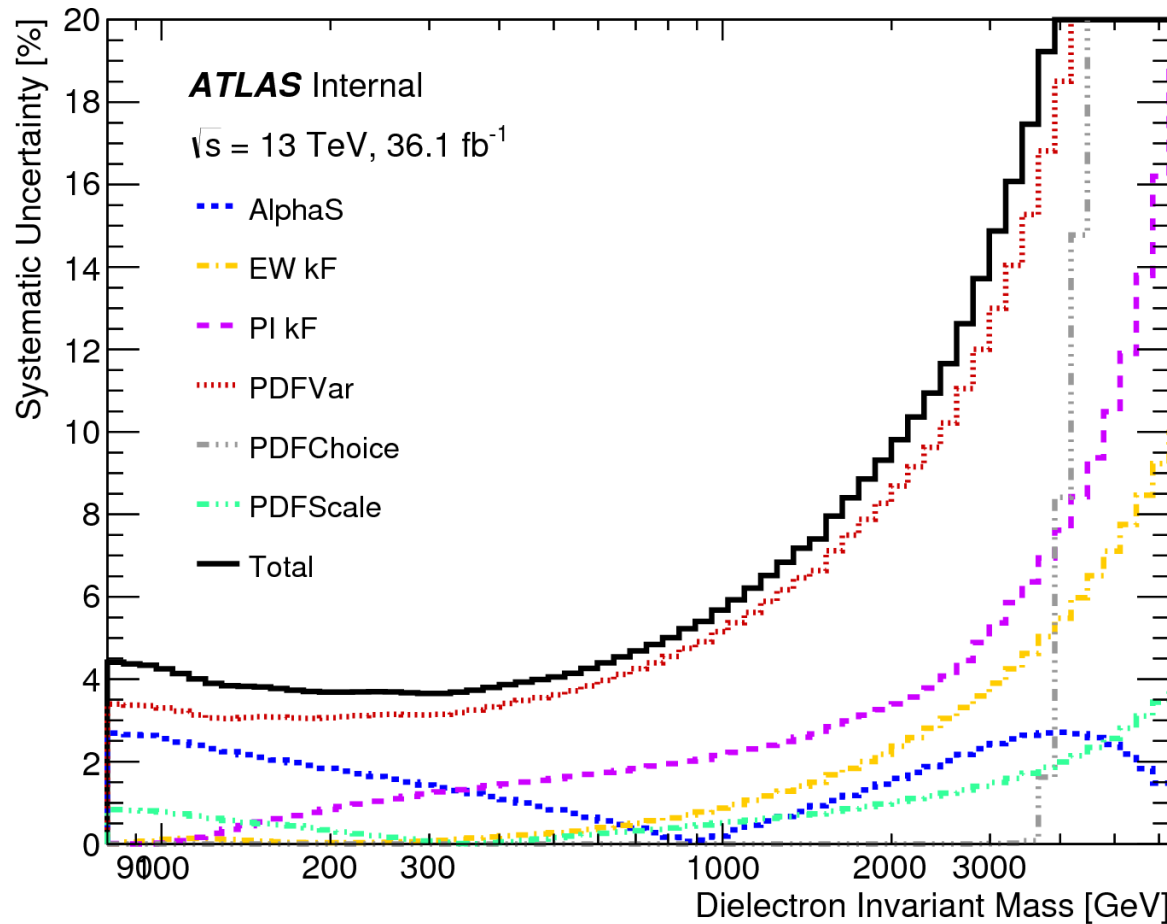
Assessment of Experimental Uncertainties

- Largest contribution from fake background extrapolation uncertainty
- Others well under control at the sub-10% level



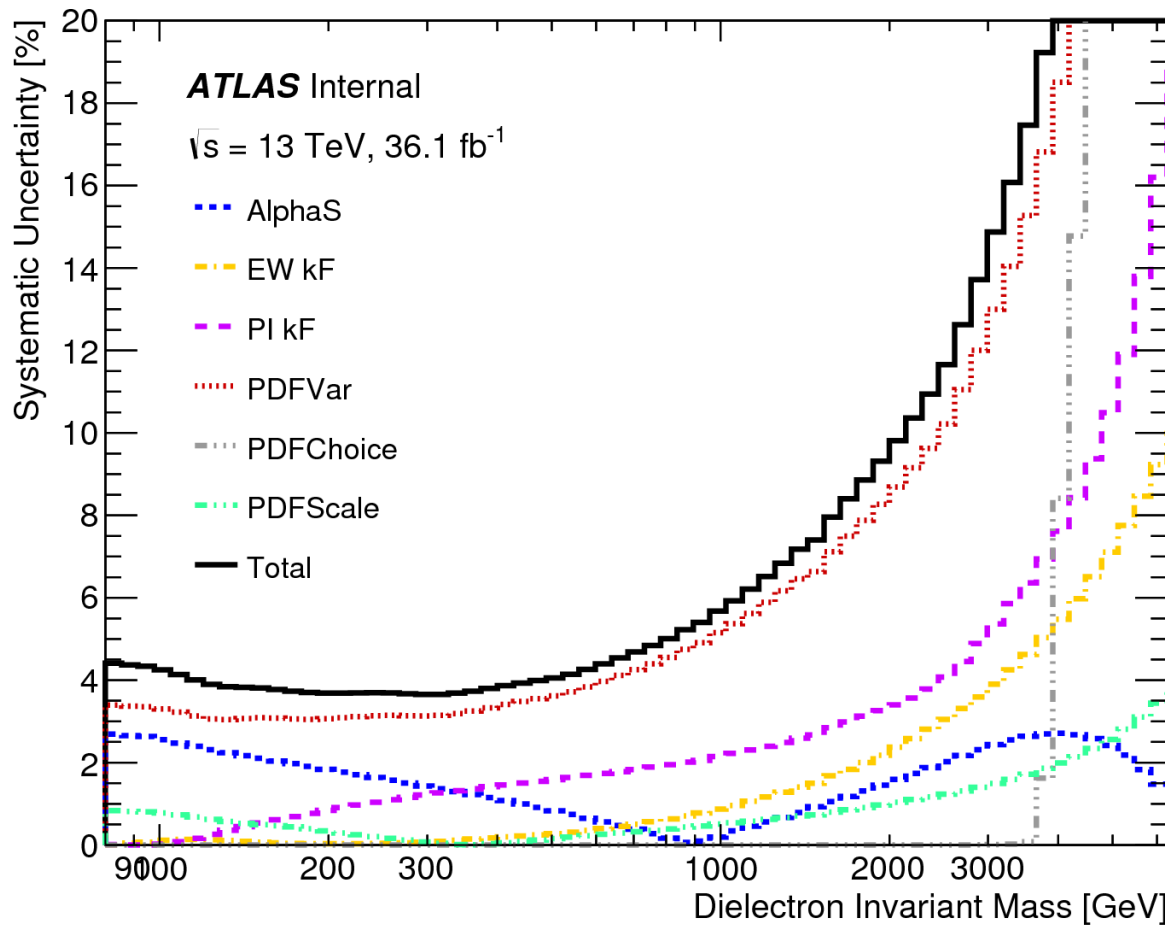
Assessment of Theoretical Uncertainties

- Largest uncertainties in analysis are theoretical, due to the PDFs!
- Others fairly well under control



Assessment of Theoretical Uncertainties

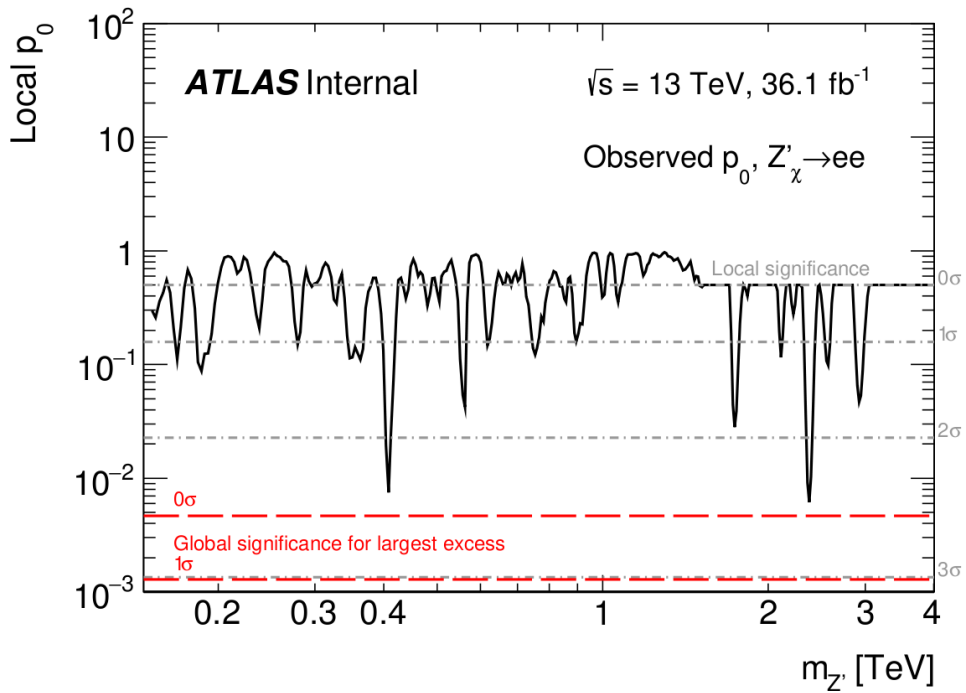
- Largest uncertainties in analysis are theoretical, due to the PDFs!
- Others fairly well under control



- Specifically 'PDFVar' and 'PDFChoice' uncertainties
 - 'PDFVar' denotes uncertainty on predicted Drell-Yan event yield due to imprecision in PDFs (19% at 4 TeV)
 - 'PDFChoice' denotes uncertainty from differing predictions of several modern PDF sets (8.4% at 4 TeV)

Performing the Search for a Signal

- Log Likelihood Ratio (LLR) test
- Binned likelihood function constructed from SM background expectation and Z'_χ signal templates
- Use likelihood to test over 500 mass-points $M_{Z'}$ (interpolated in plot below)
- Extract local p-value associated with each mass-point; global p-value from toys

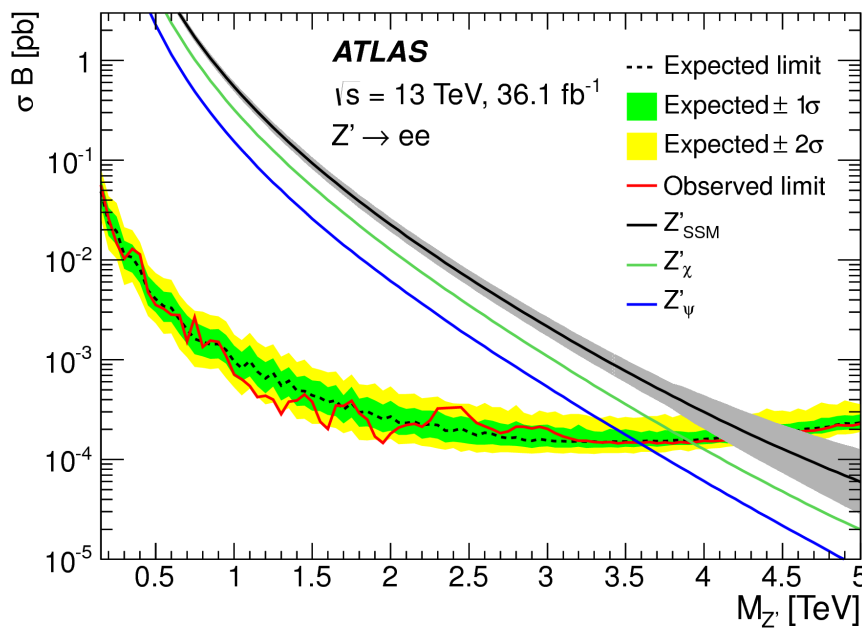


Channel	Mass [GeV]	Local p_0 [%]	Global p_0 [%]
ee	2373	0.6%	58%
$\mu\mu$	481	5.8%	91%
$\ell\ell$	2373	1.4%	83%

→ Result: no significant deviations observed during search

Setting Limits on the SSM and $E_6 Z'$ Models

- Set exclusion limits at 95% C.L. on Z' signal cross section times branching fraction (σB)
- Use Bayesian Analysis Toolkit (BAT): employs MCMC to marginalize over nuisance parameters of likelihood function
- Combined likelihood constructed from both ee and $\mu\mu$ channels → ee dominates due to higher efficiency and better resolution

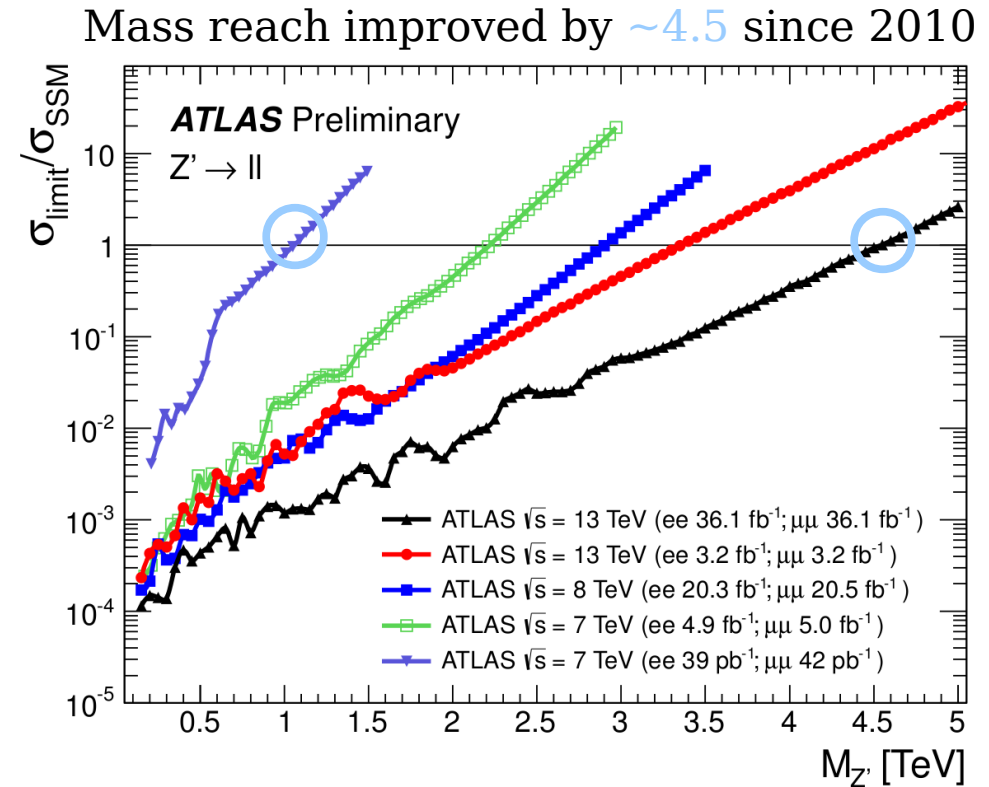


Model	Width [%]	$\theta_{E_6} [\text{Rad}]$	Lower limits on $m_{Z'} [\text{TeV}]$					
			ee		$\mu\mu$		$\ell\ell$	
			Obs	Exp	Obs	Exp	Obs	Exp
Z'_{SSM}	3.0	-	4.3	4.3	4.0	3.9	4.5	4.5
Z'_{χ}	1.2	0.50π	3.9	3.9	3.6	3.6	4.1	4.0
Z'_{S}	1.2	0.63π	3.9	3.8	3.6	3.5	4.0	4.0
Z'_{I}	1.1	0.71π	3.8	3.8	3.5	3.4	4.0	3.9
Z'_{η}	0.6	0.21π	3.7	3.7	3.4	3.3	3.9	3.8
Z'_{N}	0.6	-0.08π	3.6	3.6	3.4	3.3	3.8	3.8
Z'_{ψ}	0.5	0π	3.6	3.6	3.3	3.2	3.8	3.7

→ Result: Set some of the strongest limits to date

Dilepton Analysis Results

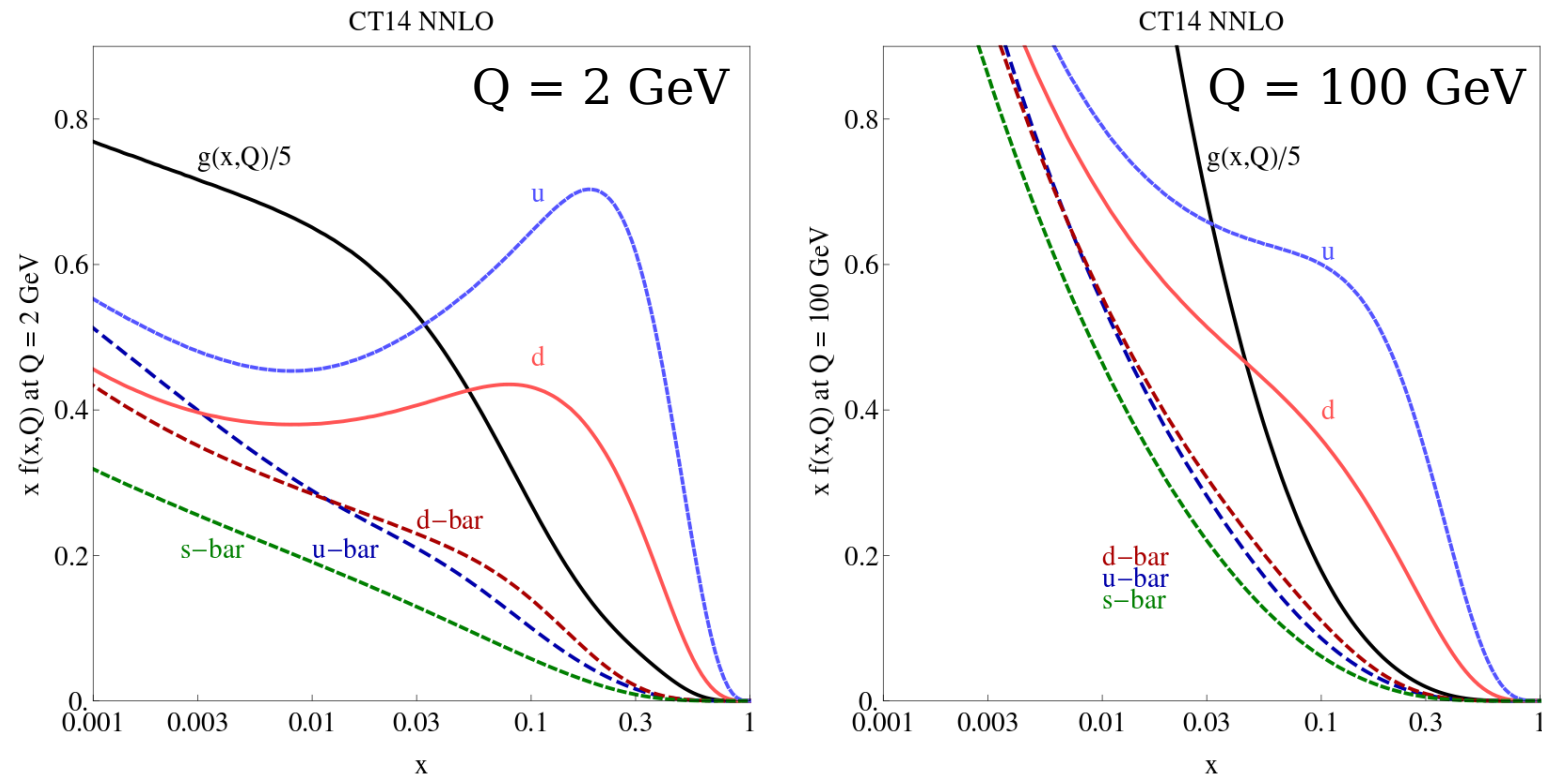
- Searched for $Z' \rightarrow e^+e^-$ production in dielectron final states using 36.1/fb dataset
 - No evidence of significant excess
- Set some of the most stringent mass limits to date
 - Lower limit of 4.5 TeV on Z'_{SSM}
 - Lower limit of 4.1 TeV on E_6 motivated Z'_χ
 - Minimal Model limits on relative coupling constant γ'



Part II: Reduction of PDF Uncertainty

What are Parton Distribution Functions?

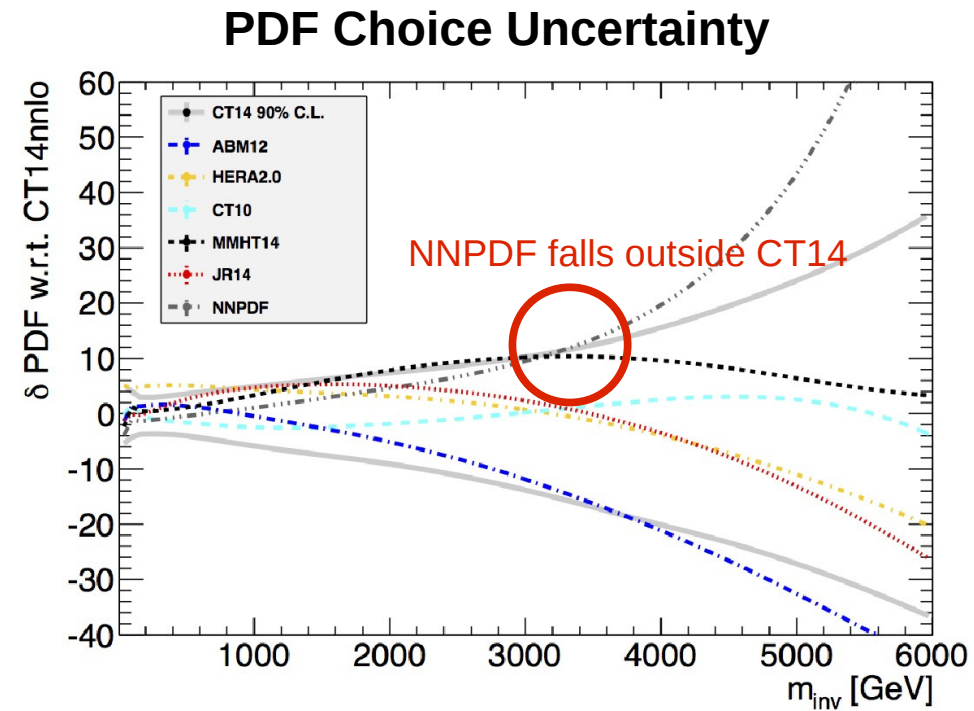
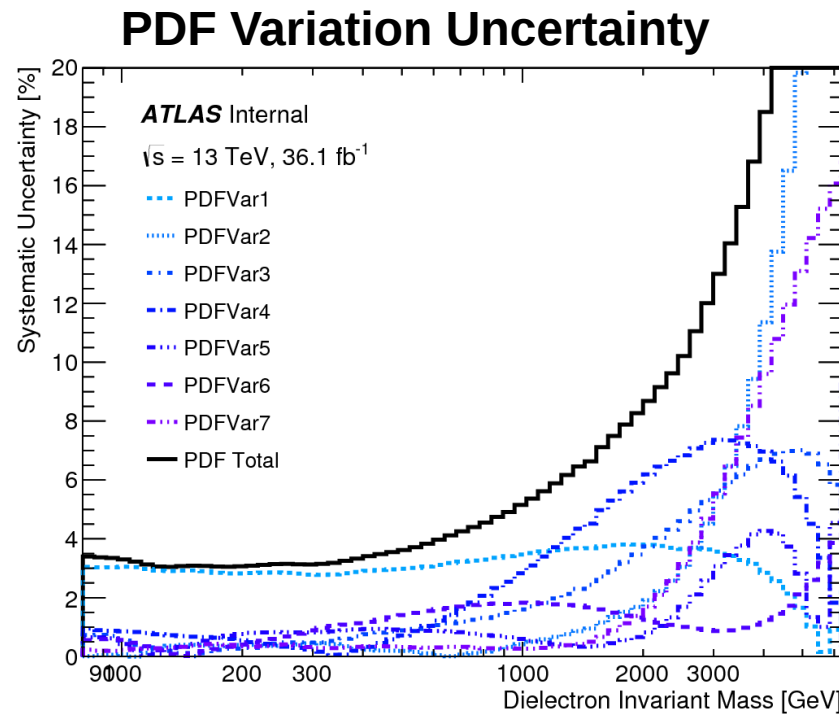
- PDFs parametrize motion of partons (quarks and gluons) within the proton
- Each parton carries momentum fraction x of total proton momentum



- Shared proton momentum depends on energy scale Q of the collision
- PDFs cannot be calculated from first principles

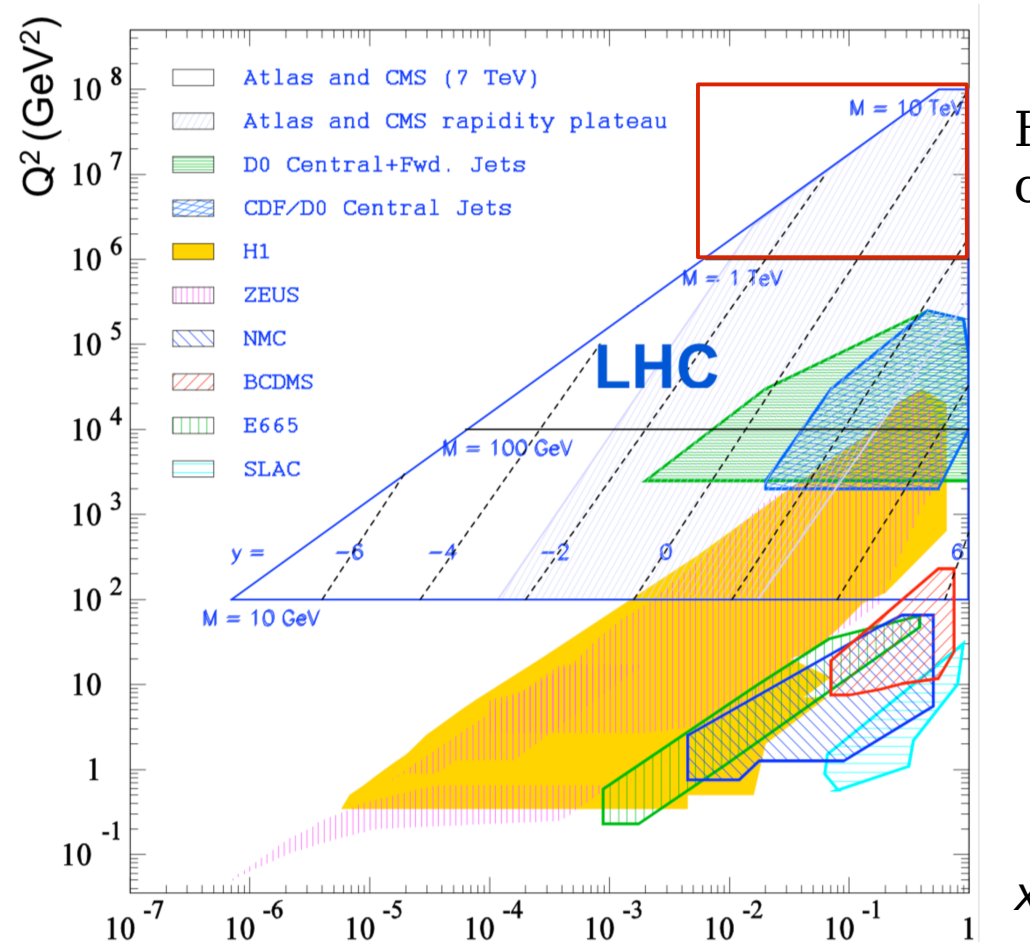
PDF Uncertainties Dominate the Dilepton Analysis

- Affect discovery potential, ability to set exclusion limits as data collected
- Loose ability to differentiate between models in discovery scenario



What can we do about it?

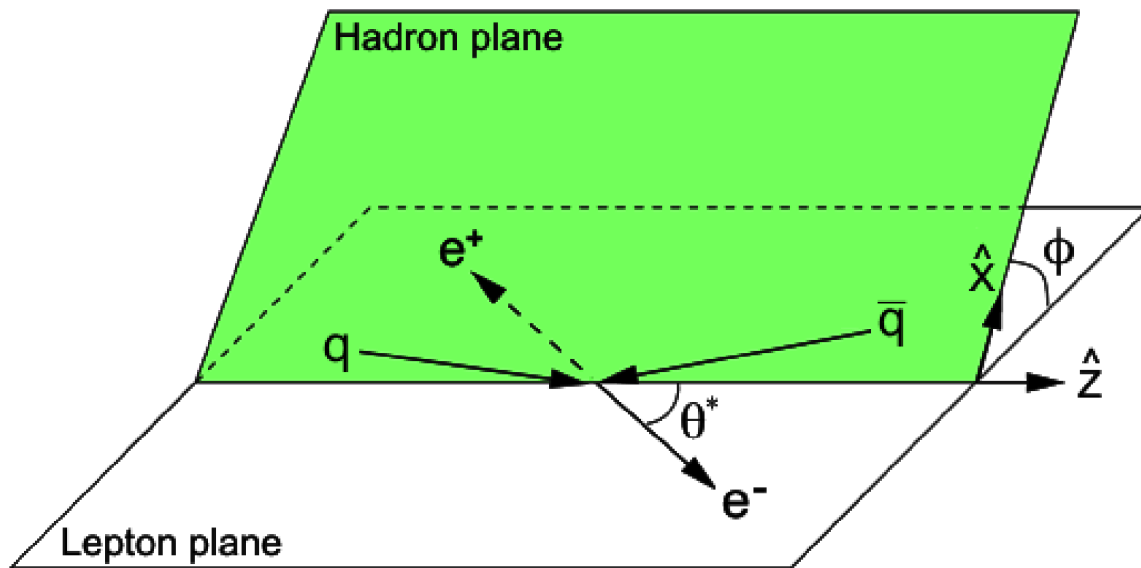
- High-mass Drell-Yan events produced in high- x $q\bar{q}$ collisions
- High- x is one of the least constrained regions of PDF parameter space
- LHC offers unique opportunity to incorporate high- x measurements into PDF global fits



High-mass search region
of Dilepton analysis

'Discovery' of $\cos\theta^*$

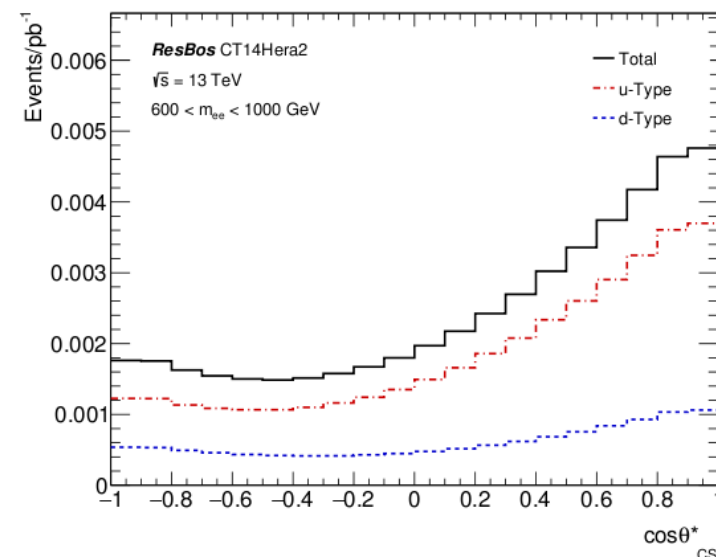
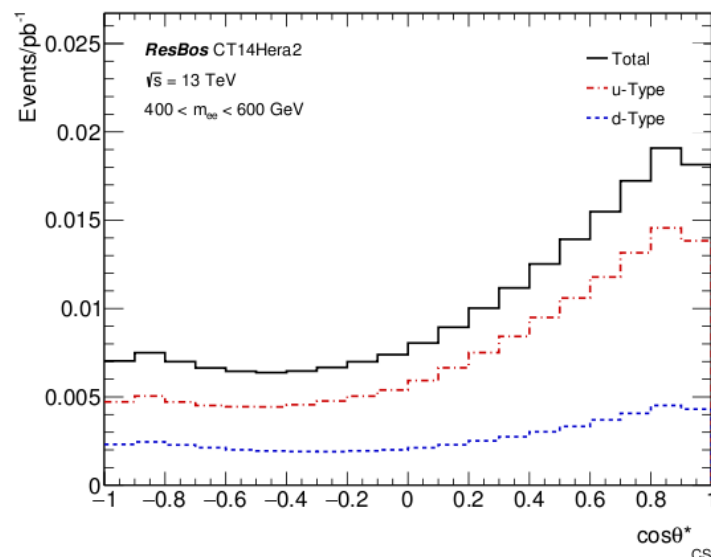
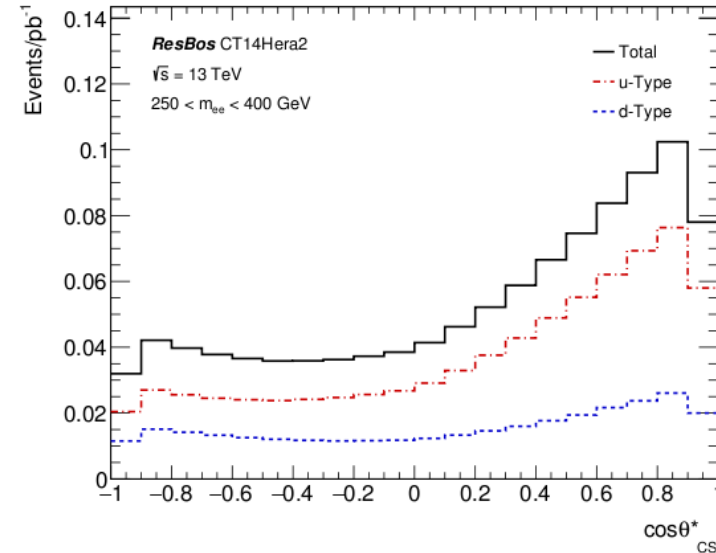
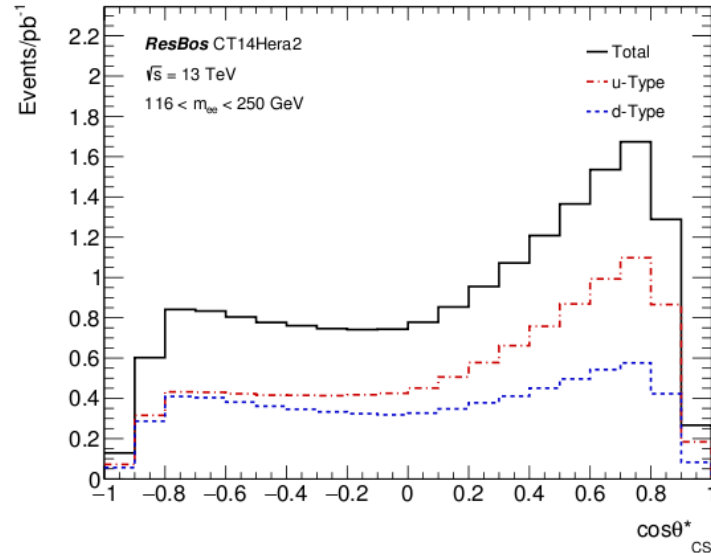
- PDF Global Fits have relied on doubly-differential Drell-Yan measurements
- Discovered inclusion of third dimension of $\cos\theta^*$ can be significant
- $\cos\theta^*$ defined as angle between outgoing lepton and incoming quark in Collins-Soper frame of reference



$$\frac{d^2\sigma}{dm_{\ell\ell} d|y_{\ell\ell}|}$$
$$\frac{d^3\sigma}{dm_{\ell\ell} dy_{\ell\ell} \cos\theta^*}$$

$\cos\theta^*$ separates u- and d-type Drell-Yan sub-processes

- Majority of Drell-Yan cross section attributed to $u\bar{u}$ initial-state for $\cos\theta^*>0$
- LHC becomes a $u\bar{u}$ collider. Let's take advantage of this fact!



But Why Do These Separations Occur?

→ Drell-Yan cross section provides an explanation

$$\frac{d^3\sigma}{dm_{\ell\ell}dy_{\ell\ell}\cos\theta^*} = \frac{\pi\alpha^2}{3m_{\ell\ell}s} \sum_q P_q \left[f_{q/P_1}(x_1, Q^2) f_{\bar{q}/P_2}(x_2, Q^2) + (q \leftrightarrow \bar{q}) \right]$$

But Why Do These Separations Occur?

→ Drell-Yan cross section provides an explanation

$$\frac{d^3\sigma}{dm_{\ell\ell}dy_{\ell\ell}\cos\theta^*} = \frac{\pi\alpha^2}{3m_{\ell\ell}s} \sum_q P_q \left[f_{q/P_1}(x_1, Q^2) f_{\bar{q}/P_2}(x_2, Q^2) + (q \leftrightarrow \bar{q}) \right]$$

→ C_q are *functions* of dilepton mass and electroweak parameters; result in slightly different behavior for u - and d -type quarks.

$$P_q = C_q^0 \left(1 + \cos^2 \theta^* \right) + C_q^1 \cos \theta^*$$

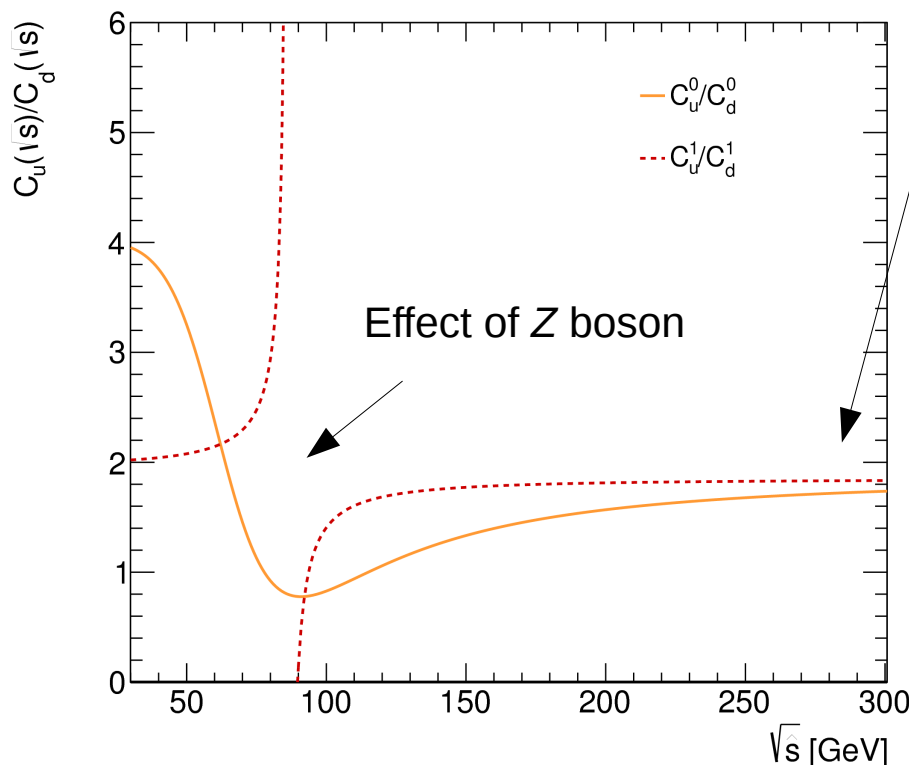
But Why Do These Separations Occur?

→ Drell-Yan cross section provides an explanation

$$\frac{d^3\sigma}{dm_{\ell\ell}dy_{\ell\ell}\cos\theta^*} = \frac{\pi\alpha^2}{3m_{\ell\ell}s} \sum_q P_q \left[f_{q/P_1}(x_1, Q^2) f_{\bar{q}/P_2}(x_2, Q^2) + (q \leftrightarrow \bar{q}) \right]$$

→ C_q are *functions* of dilepton mass and electroweak parameters; result in slightly different behavior for u - and d -type quarks.

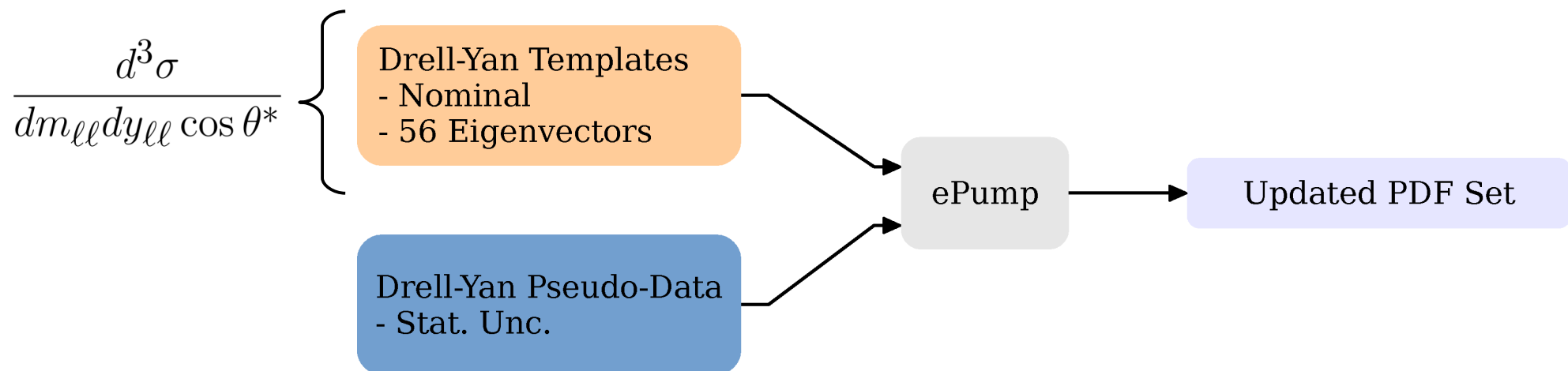
$$P_q = C_q^0 \left(1 + \cos^2 \theta^* \right) + C_q^1 \cos \theta^*$$



- Ratios between coefficients asymptote as \sqrt{s} increases
- C_u^0/C_d^0 explains u -type dominance as function of mass
- C_u^1/C_d^1 explains u -type dominance in $\cos\theta^* > 0$ region

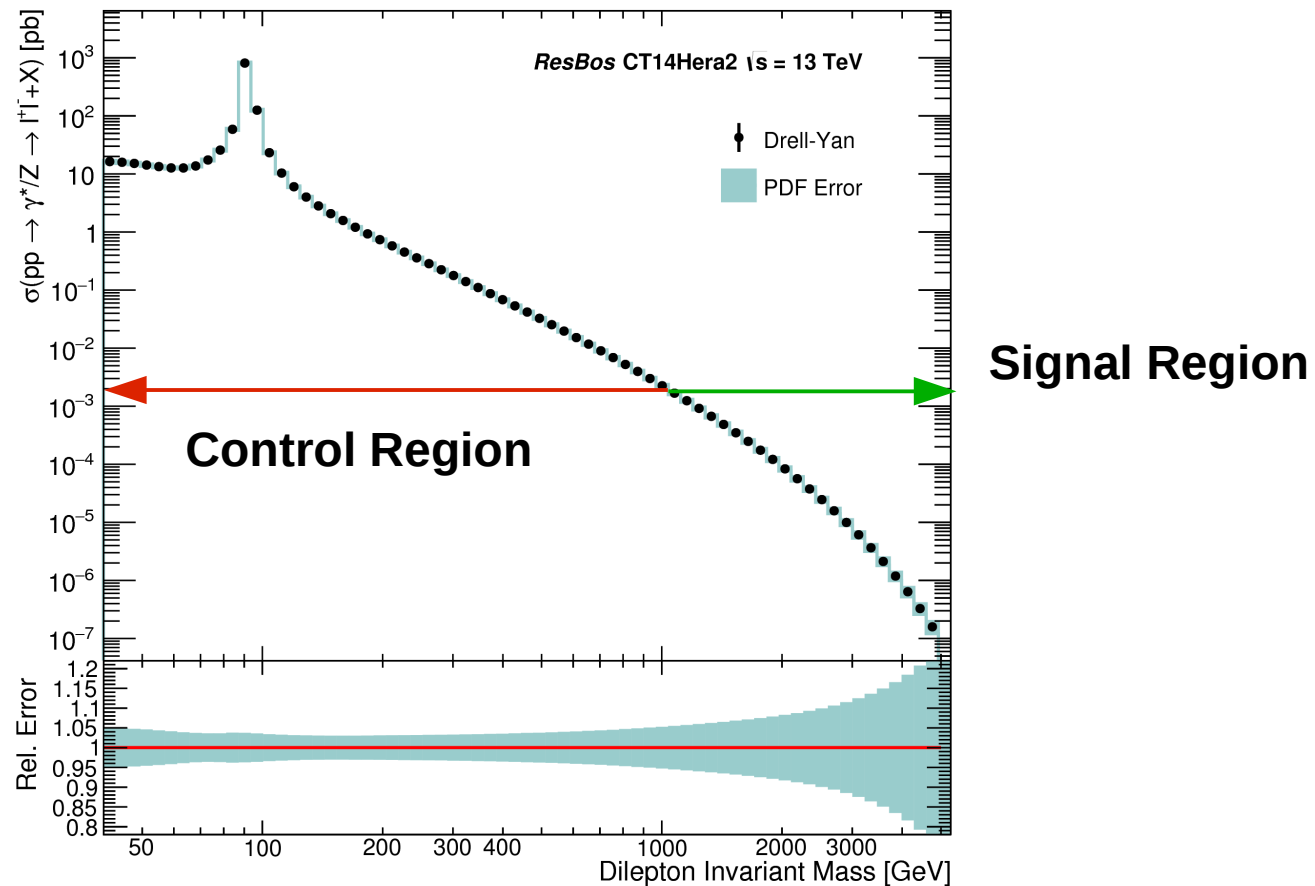
How to Reduce the current PDF Uncertainty

- Use ePump to emulate a future PDF global fit
- Incorporate *simulated* LHC Drell-Yan data (i.e. pseudo-data) into updated fit
- Specifically take advantage of new and potentially useful dimension of $\cos\theta^*$



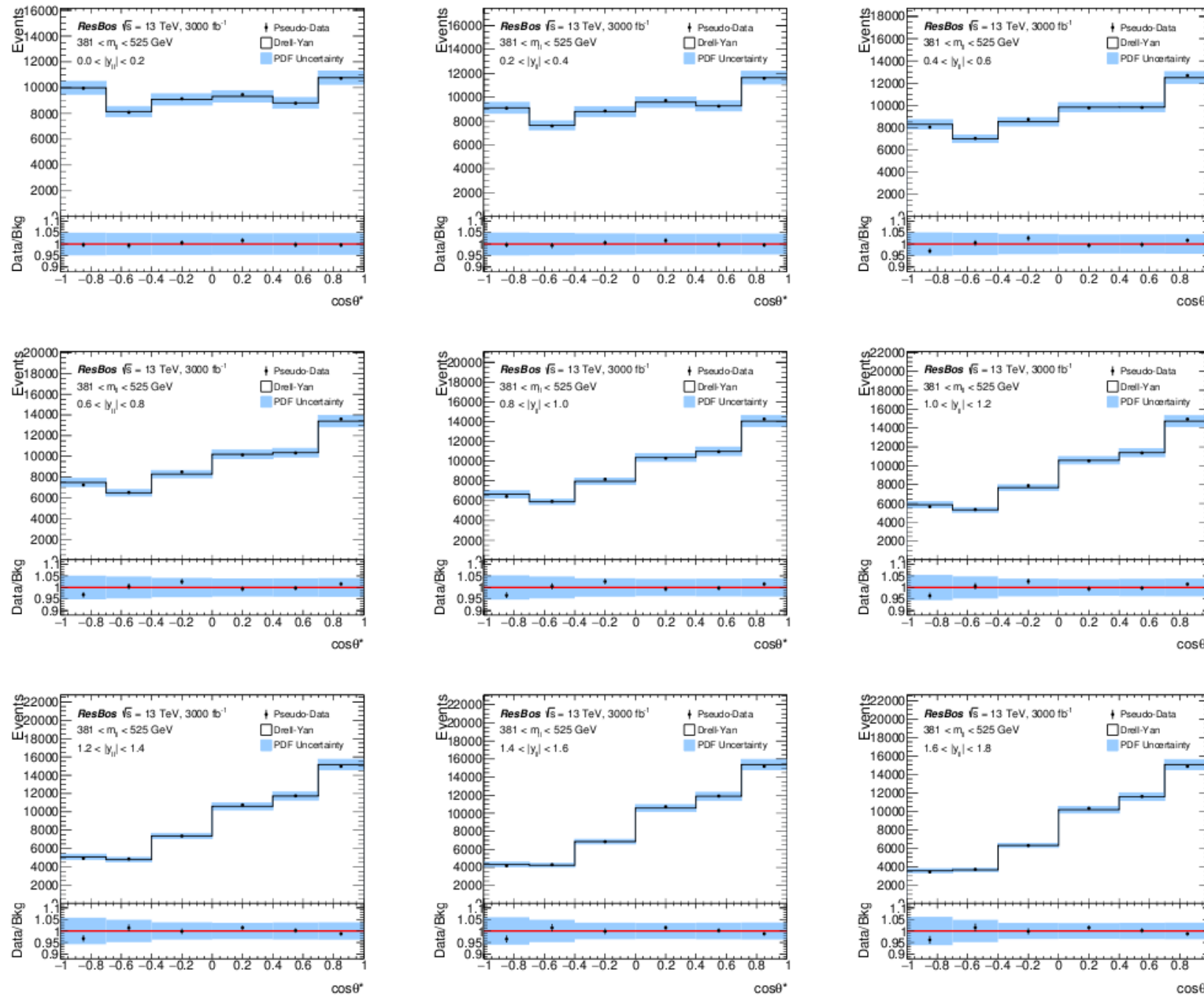
Strategy for the PDF Update with ePump

- Define two regions of dilepton mass: **control** region and **signal** region
- Perform PDF update using using ePump templates in control region (defined on $40 < m_{ll} < 1000$, $|y_{ll}| < 3.6$, $-1 < \cos\theta^* < 1$)
- Assess impact on PDF uncertainty in signal region



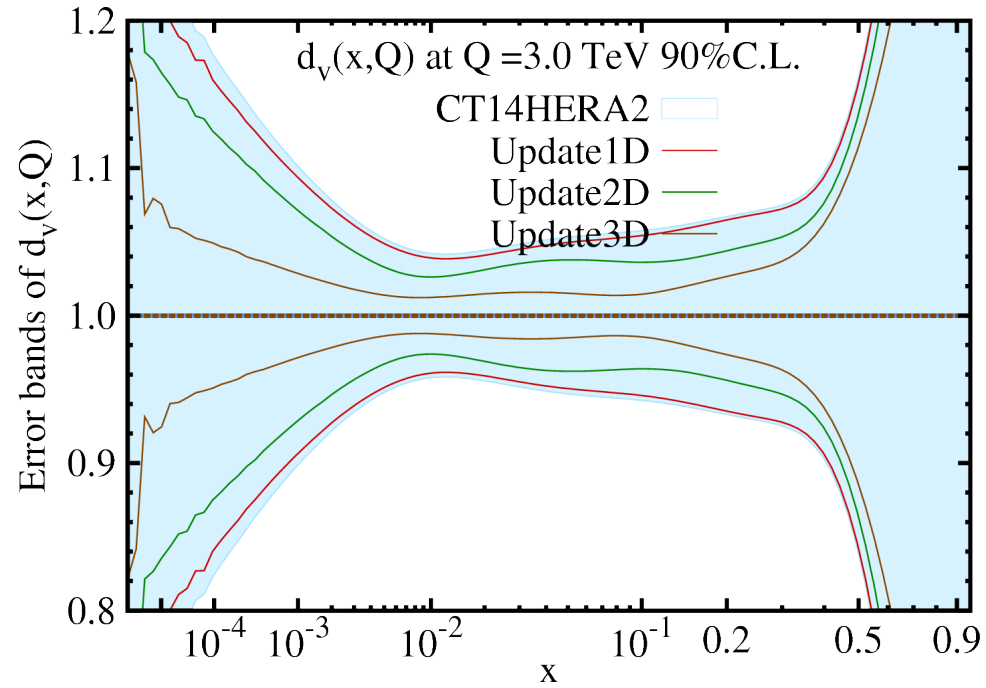
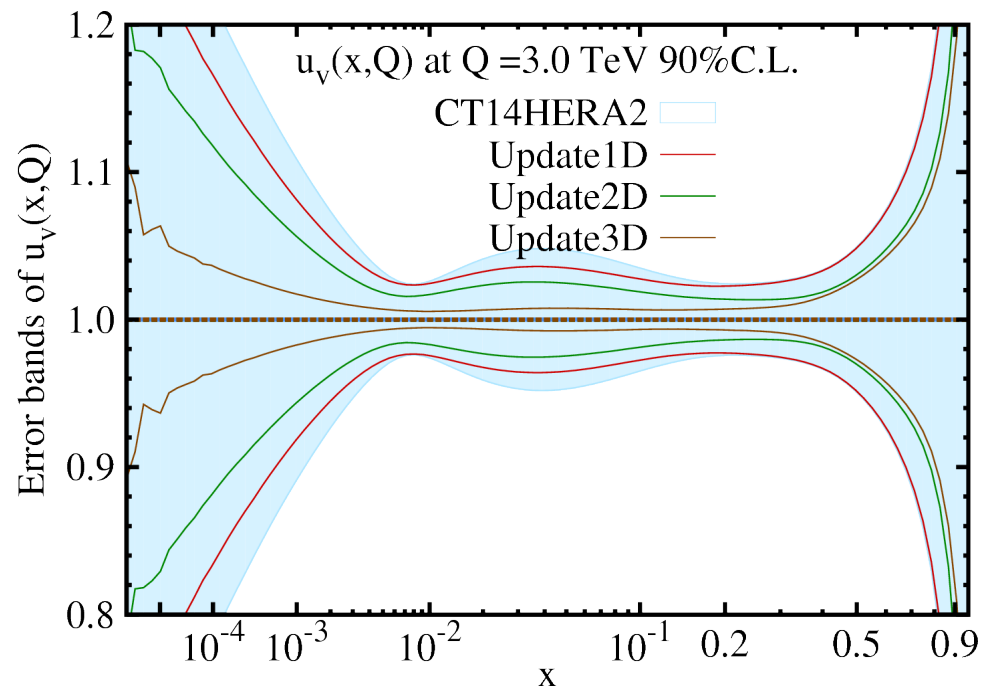
ePump Templates constructed triple-differentially

→ In slices of m_{ll} , $|y_{ll}|$, $\cos\theta^*$, 1296 bins total, pseudo-data generated at 3000/fb



Update Impact on Valence PDFs

- Assess impact on $u_v(x)$ and $d_v(x)$ valence quark PDFs
- At $x=0.3$, $u_v(x)$ is reduced from 2.6% to 0.9%, $d_v(x)$ from 7.5% to 3.6%

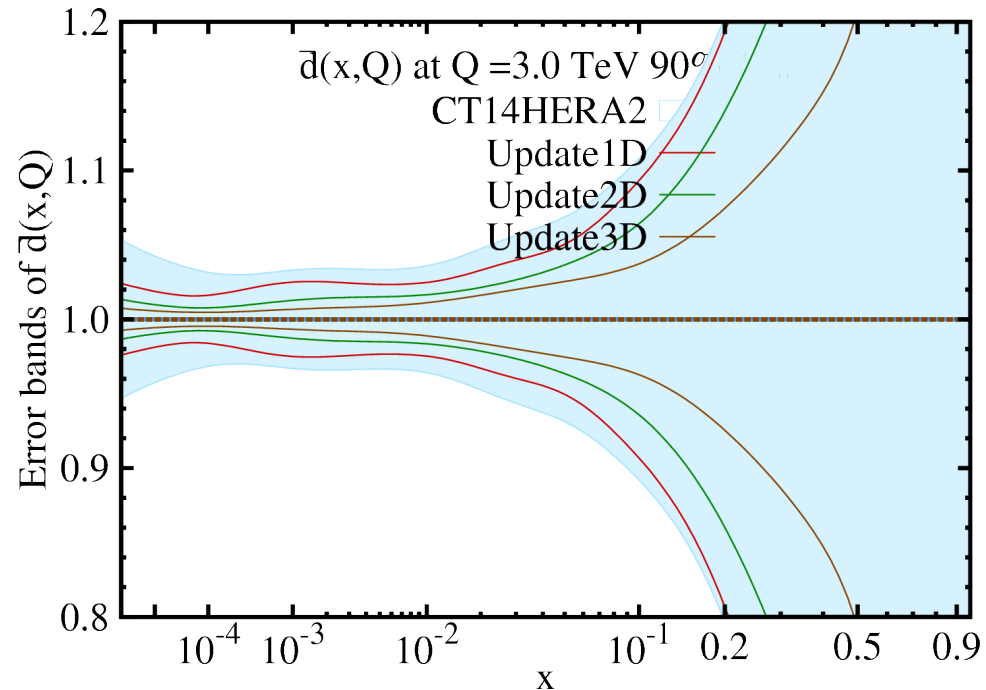
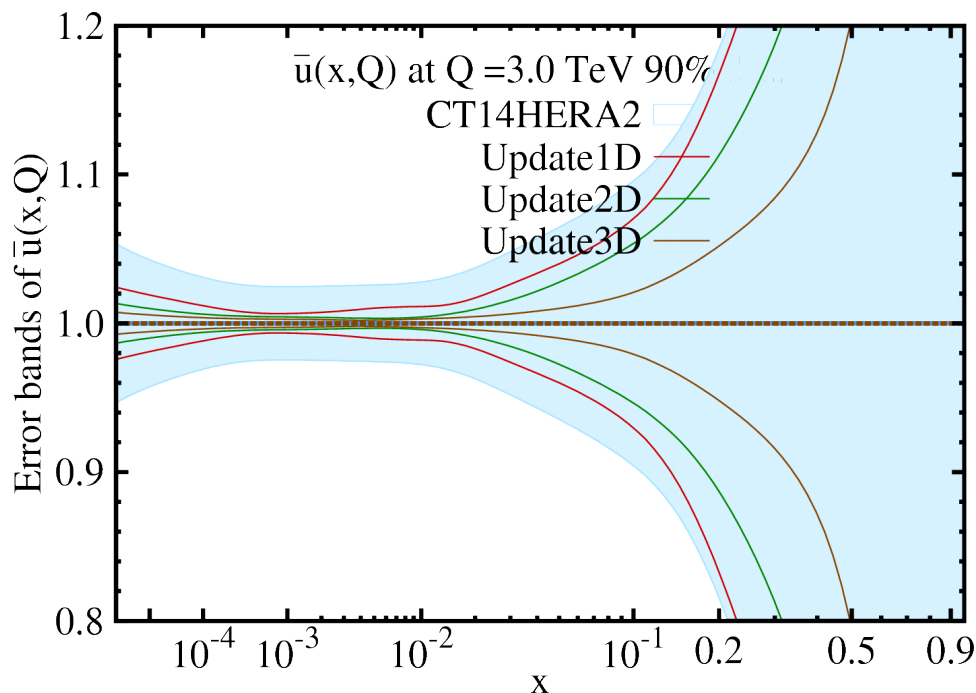


- 1D for mass-only, 2D for mass+rapidity, 3D for mass+rapidity+ $\cos\theta^*$ templates

- Inclusion of Drell-Yan pseudo-data into global fit dramatically improves precision of PDFs in high- x regions of interest

Update Impact on Sea PDFs

- Assess impact on $\bar{u}(x)$ and $\bar{d}(x)$ sea quark PDFs
- At $x=0.3$, $\bar{u}(x)$ is reduced from 30% to 8.3%, $\bar{d}(x)$ from 32% to 11%

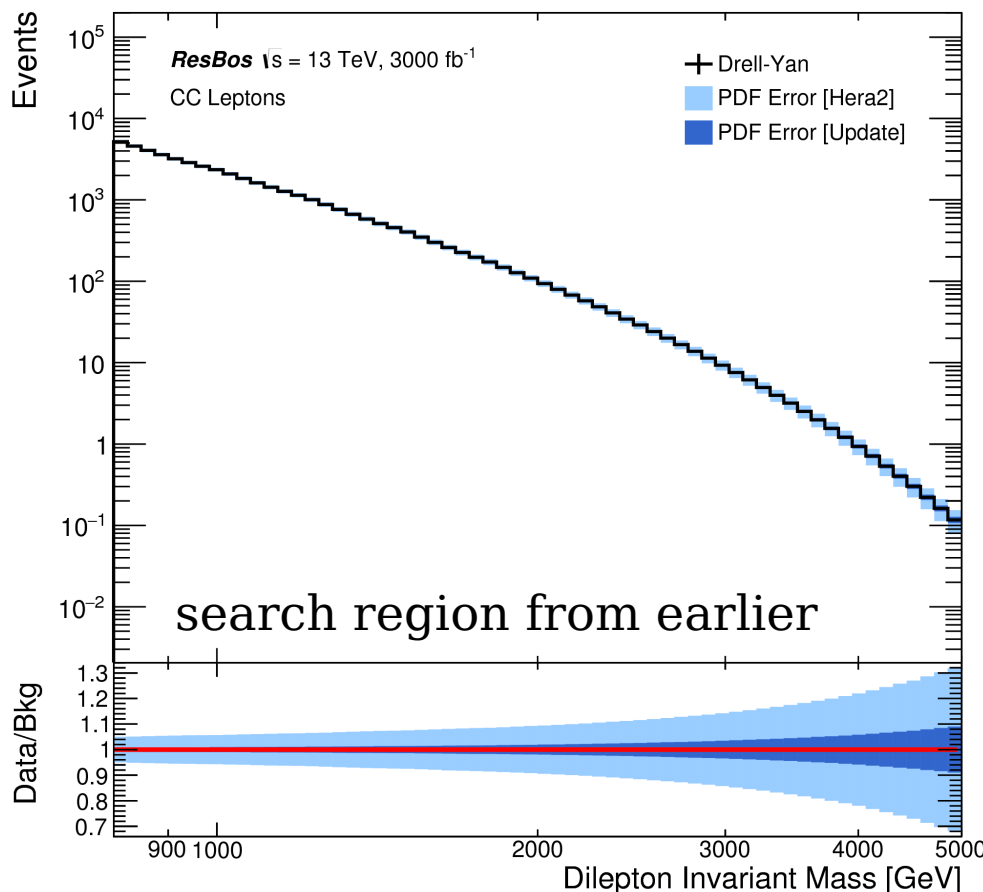


- 1D for mass-only, 2D for mass+rapidity, 3D for mass+rapidity+ $\cos\theta^*$ templates

- Inclusion of Drell-Yan pseudo-data into global fit dramatically improves precision of PDFs in high- x regions of interest

Update Impact on high-mass Drell-Yan

→ Use ePump to propagate updated PDF uncertainties to description of high-mass Drell-Yan spectrum



- At $m_{ll} = 5$ TeV, PDF uncertainty reduced from 31% to 8.9%
 - At $m_{ll} = 3$ TeV, PDF uncertainty reduced from 15% to 3.7%
 - PDF uncertainties reduced below current dilepton experimental uncertainties
 - Also performed update at 300/fb:
 - 31% to 19% at $m_{ll} = 3$ TeV
 - 15% to 7.1% at $m_{ll} = 5$ TeV

Conclusion of PDF Update

$m_{\ell\ell}$ [TeV]	PDF Update δ_{post}^{PDF} [%]	Dilepton Analysis				
		δ^{PDF} [%]	δ^{Choice} [%]	δ^{Theory} [%]	δ^{Exp} [%]	δ^{Total} [%]
1	1.0	5.4	0.0	5.9	7.7	9.7
2	2.0	8.7	0.0	9.8	11	15
3	3.7	13	0.0	15	12	19
4	6.0	19	8.4	23	13	26
5	8.9	29	47	57	14	59

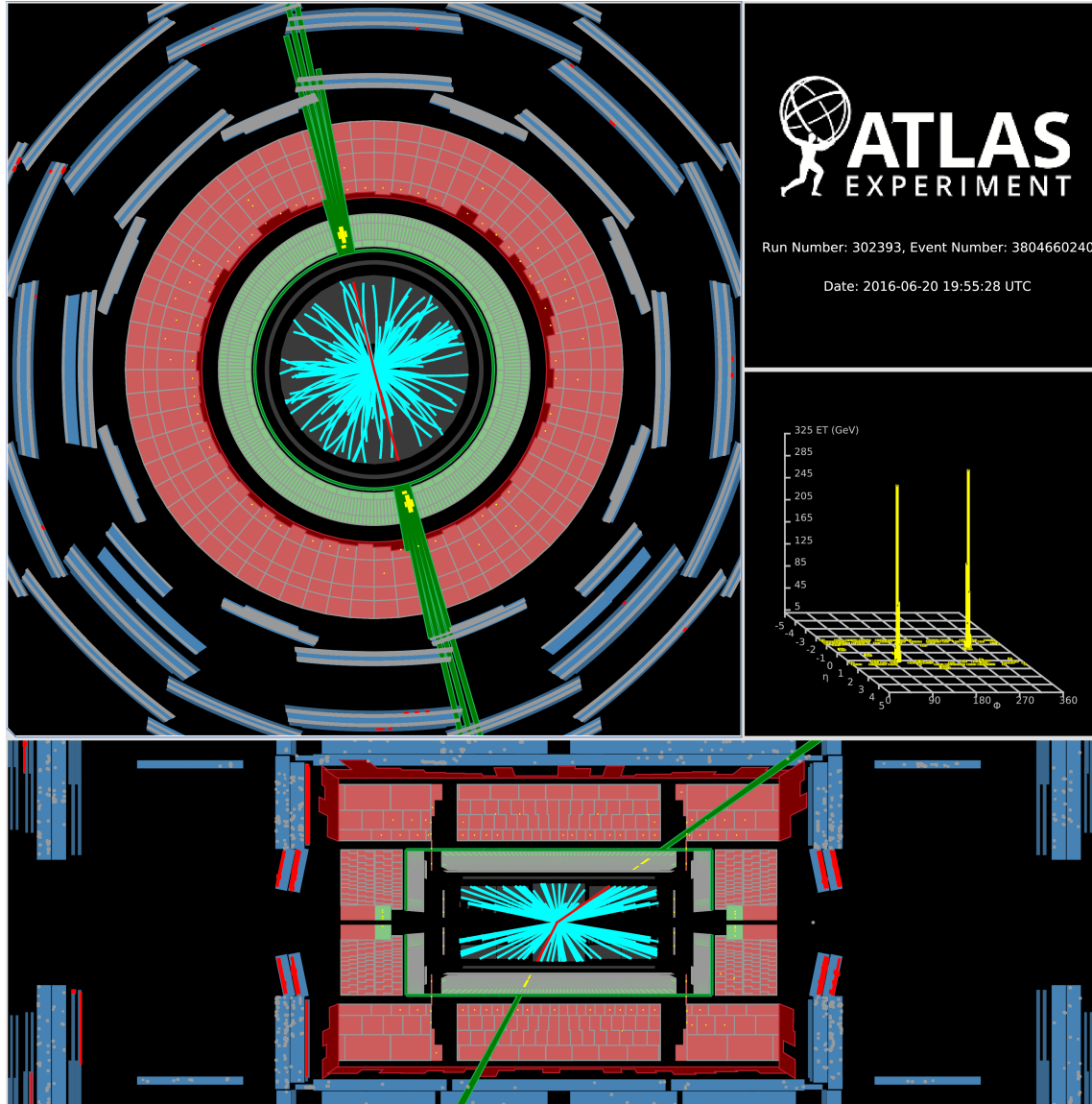
- Substantial improvement still possible for PDF uncertainties (use of $\cos\theta^*$ is crucial!)
- Suggest a re-assessment of the 'PDFChoice' uncertainty, improving future dilepton search discovery potential and model discrimination ability

Final Thoughts

- Huge thanks to my adviser Chip Brock
- Thanks for your attention
- Any Questions?

Extra

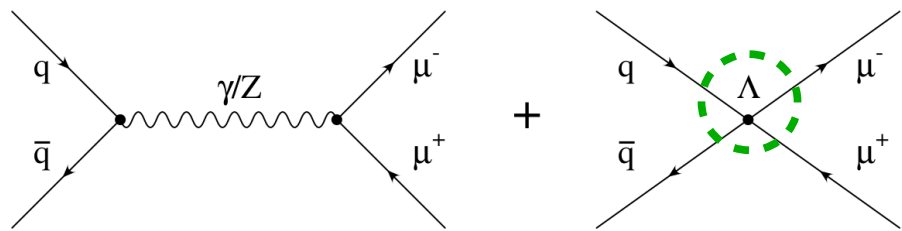
Dielectron Event Display



- Mass of Dielectron Event: 2.38 TeV
- Leading electron has an E_T of 889 GeV, and an η of -0.51
- Subleading electron has an E_T of 868 GeV, and an η of 1.14

Non-Resonant Dilepton Models

$$\frac{d\sigma}{dm_{\ell\ell}} = \frac{d\sigma_{DY}}{dm_{\ell\ell}} - \eta_{XY} \frac{F_I}{\Lambda^2} + \frac{F_C}{\Lambda^4}$$

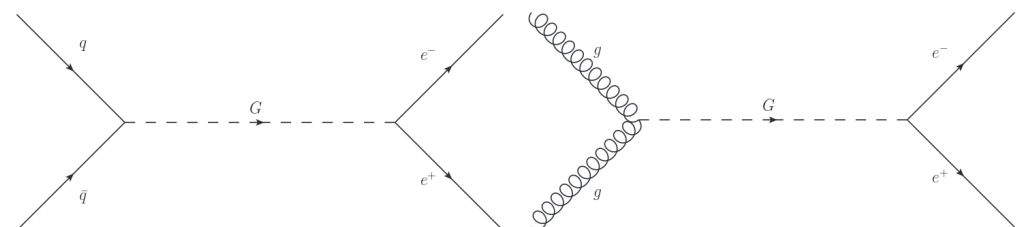


Contact-Interactions

- Quark and Lepton Compositeness
- 2
 - Λ defines Compositeness Scale
 - η_{xy} defines the chiral structure of interaction → interference
 - Signal appears as broad excess above SM expectation

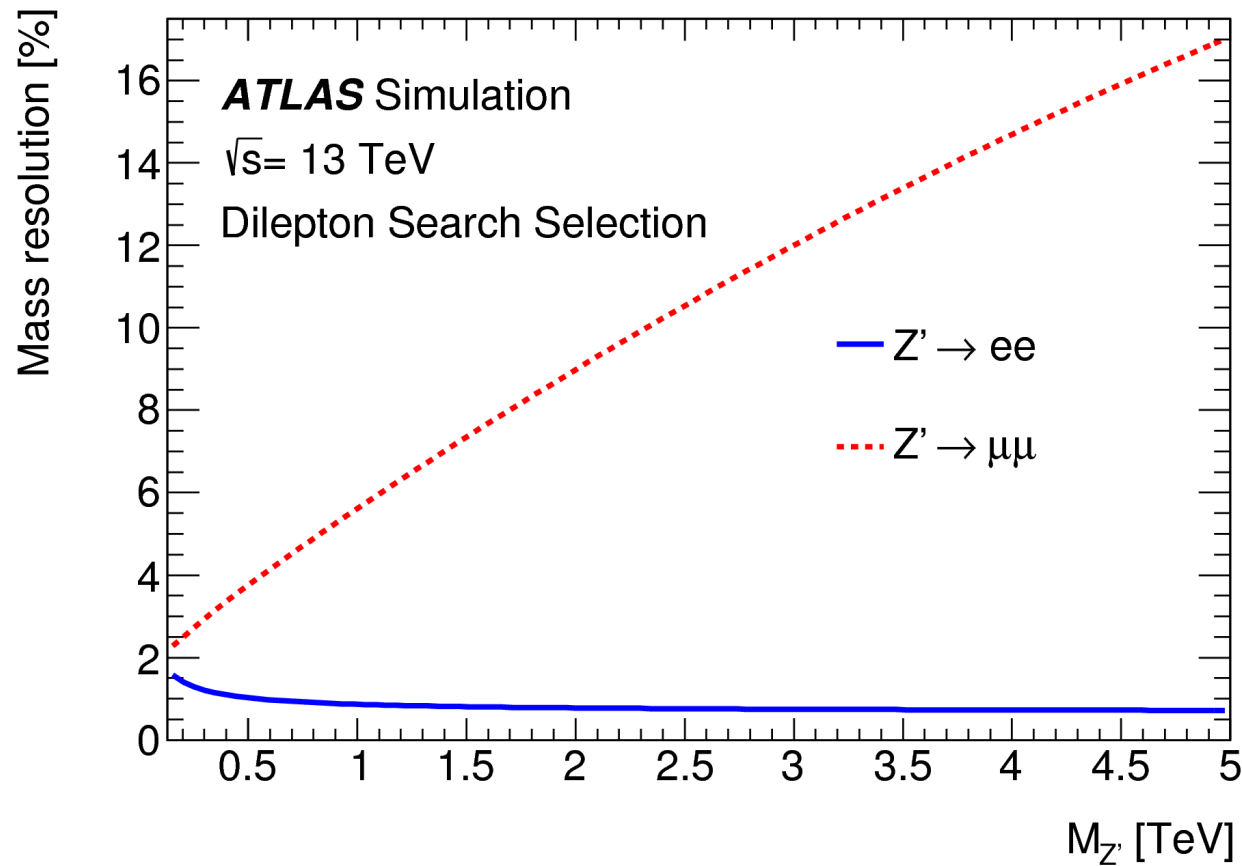
ADD Graviton

- Solution to Hierarchy Problem
 - Large extra dimensions
 - KK modes → almost continuous spectrum
 - M_S sets scale of quantum gravity
 - F is dependence on extra dimension assumptions



$$\frac{d\sigma}{dm_{\ell\ell}} = \frac{d\sigma_{DY}}{dm_{\ell\ell}} + \mathcal{F} \frac{F_I}{M_S^4} + \mathcal{F}^2 \frac{F_G}{M_S^8}$$

Dilepton Mass Resolution



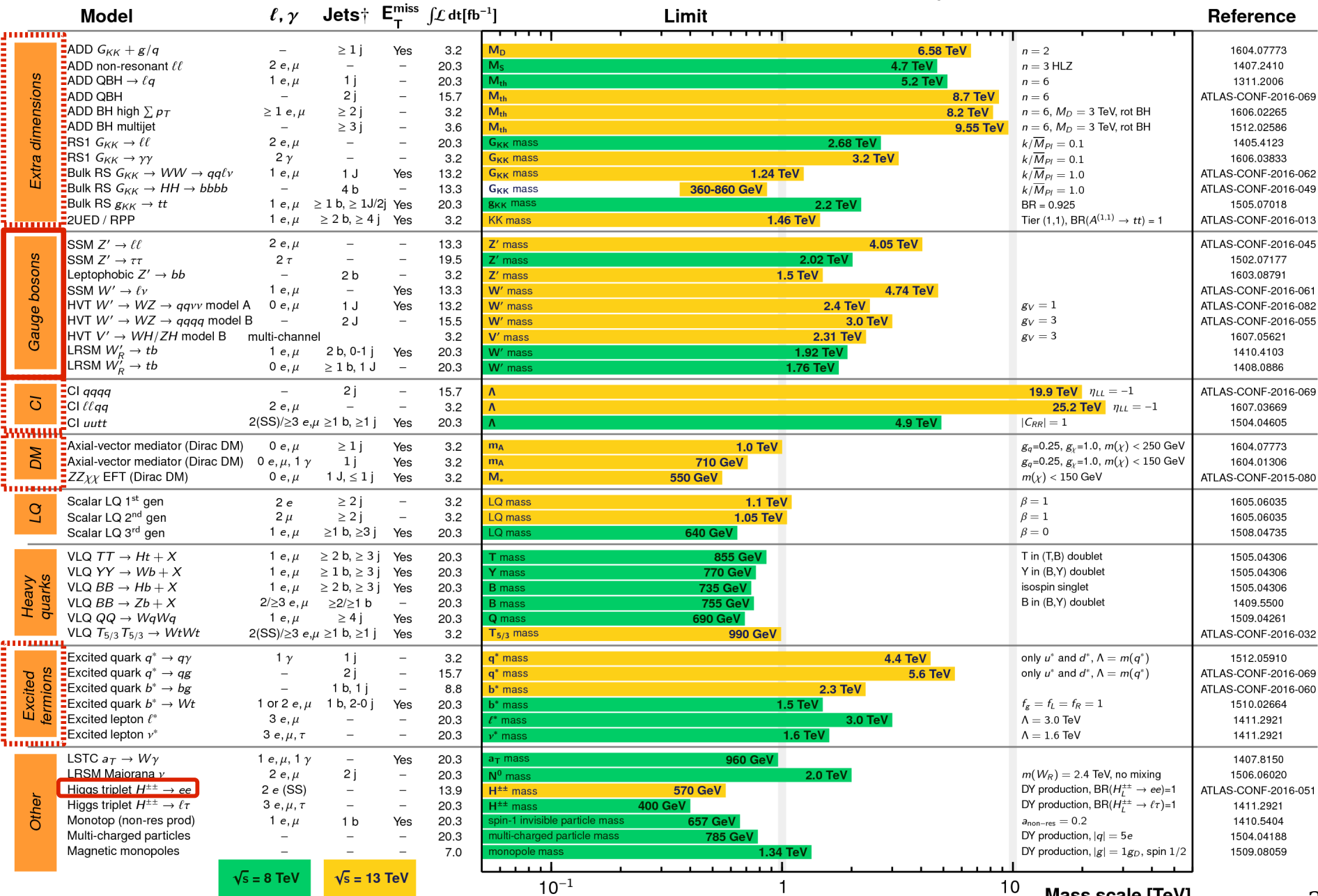
ATLAS Exotics Searches* - 95% CL Exclusion

Status: August 2016

ATLAS Preliminary

$$\int \mathcal{L} dt = (3.2 - 20.3) \text{ fb}^{-1}$$

$$\sqrt{s} = 8, 13 \text{ TeV}$$



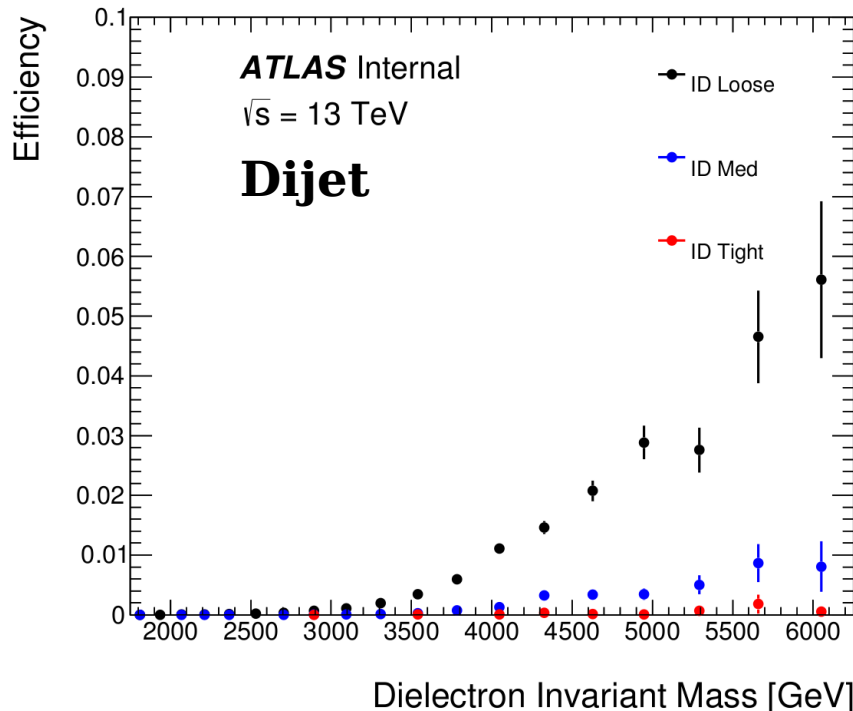
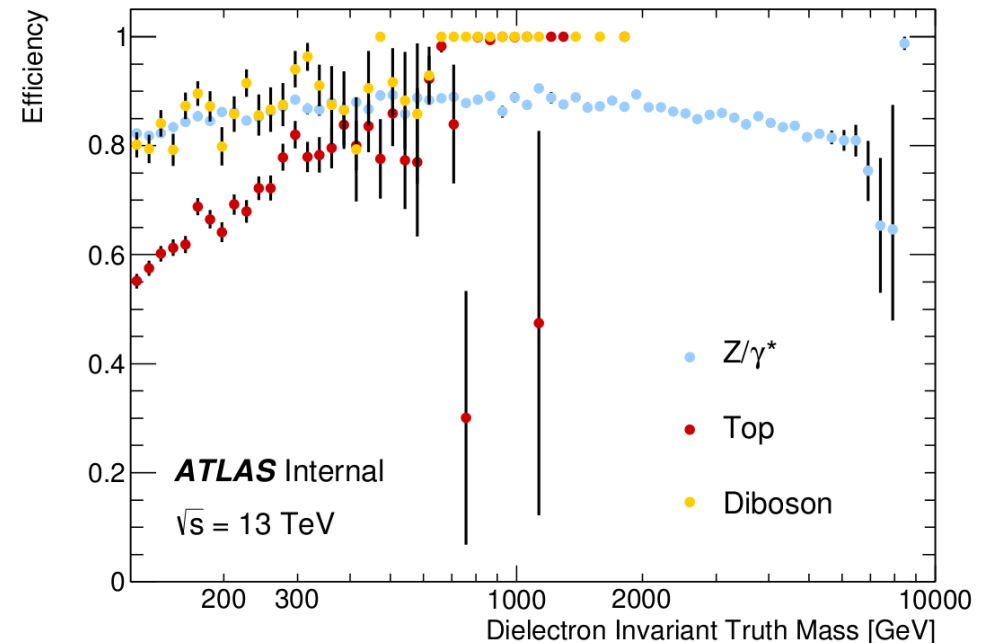
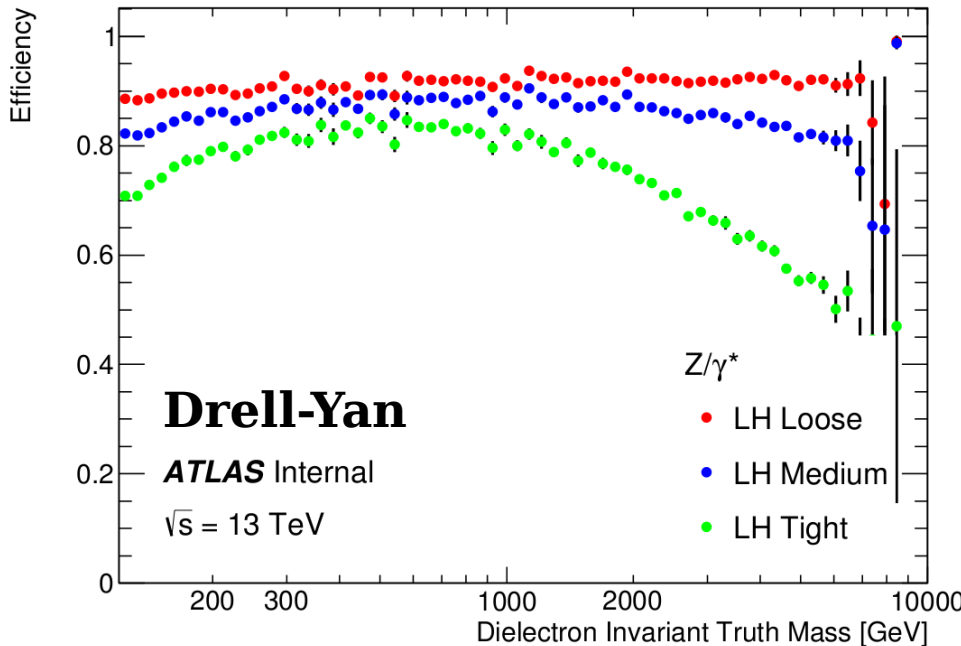
*Only a selection of the available mass limits on new states or phenomena is shown. Lower bounds are specified only when explicitly not excluded.

†Small-radius (large-radius) jets are denoted by the letter j (J).

Simulation Samples

Backgrounds	Generator	Order	Parton Shower	PDF	Notes
Z → ee/μμ	Powheg v2	NLO	Pythia 8.186	CT10	Unbinned
Drell-Yan	Powheg v2	NLO	Pythia 8.186	CT10	Mass-Binned: 120 - 5000+ GeV
Top (t̄t, single)	Powheg v2	NLO	Pythia 6.428	CT10	Unbinned
Diboson (WW, WZ, ZZ)	Sherpa 2.1.1	NLO	Sherpa 2.1.1	CT10	Mass-Binned
Signals	Generator	Order	Parton Shower	PDF	Samples
Drell-Yan	Pythia 8.186	LO	Pythia 8.186	NNPDF23LO	Mass-Binned: 70 - 5000+ GeV (for signal reweighting)
Z' (E₆ Chi)	Pythia 8.186	LO	Pythia 8.186	NNPDF23LO	Unbinned, no interference: 2, 3, 4, 5 TeV

Electron Identification



- Assess quality of Electron ID Working Points
 - Top left:** DY ID Efficiency for different working points
 - Top right:** LH Medium ID Efficiency vs. invariant mass for backgrounds
 - Bottom left:** Dijet ID Efficiency for different working points

Systematic Uncertainties

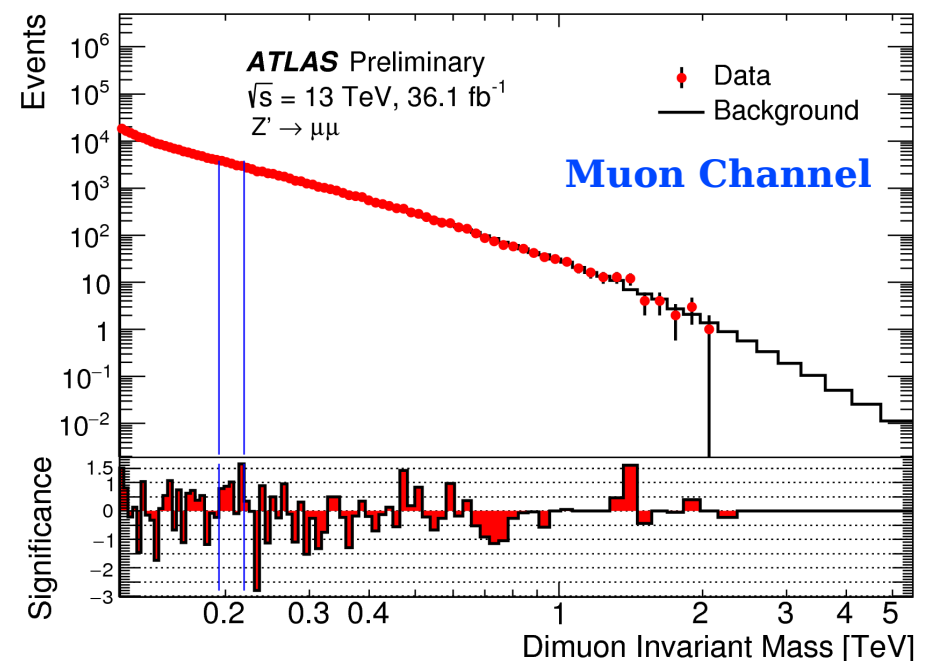
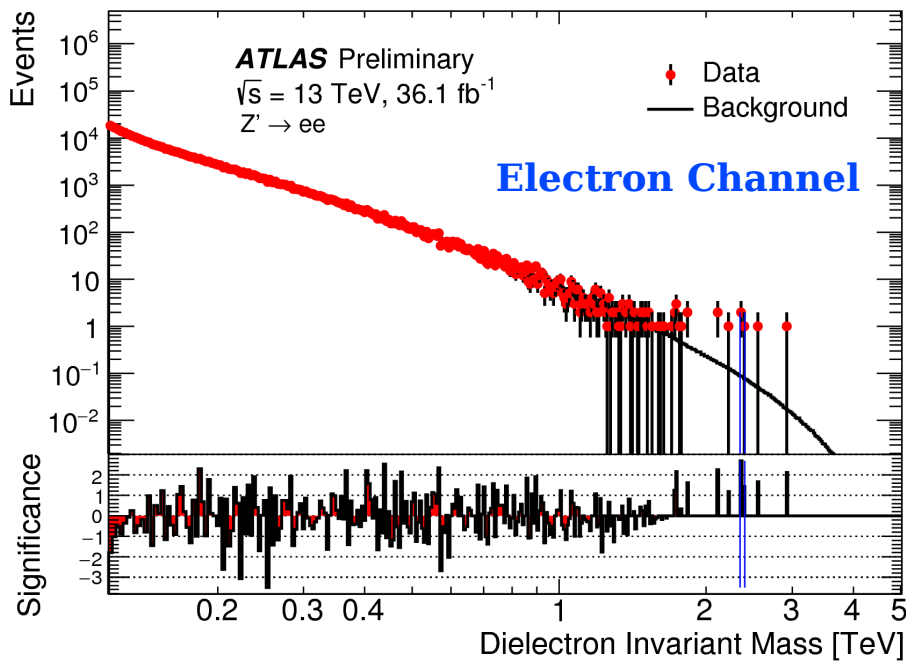
→ Shown are relative systematic uncertainties on the Z' signal and Standard Model background estimates at an invariant mass of 2 and 4 TeV

- **Background:** relative systematic uncertainty in total number of expected events in m_{ee} at 2 (4) TeV
- **Signal:** FWHM of Z'_χ with pole mass of 2 (4) TeV
- **Largest Theory Uncertainty:** PDF Variation
- **Largest Experimental Uncertainty:** Fake background estimate

Source	m_{ee} at 2 TeV [%]		m_{ee} at 4 TeV [%]	
	Signal	Background	Signal	Background
Luminosity	3.2	3.2	3.2	3.2
MC statistical	<1.0	<1.0	<1.0	<1.0
Beam energy	2.0	2.0	4.1	4.1
Pile-up effects	<1.0	<1.0	<1.0	<1.0
DY PDF choice	N/A	<1.0	N/A	8.4
DY PDF variation	N/A	8.7	N/A	19
DY PDF scales	N/A	1.0	N/A	2.0
DY α_S	N/A	1.6	N/A	2.7
DY EW corrections	N/A	2.4	N/A	5.5
DY PI corrections	N/A	3.4	N/A	7.6
Top quarks theoretical	N/A	<1.0	N/A	<1.0
Dibosons theoretical	N/A	<1.0	N/A	<1.0
Reconstruction efficiency	<1.0	<1.0	<1.0	<1.0
Isolation efficiency	9.1	9.1	9.7	9.7
Trigger efficiency	<1.0	<1.0	<1.0	<1.0
Identification efficiency	2.6	2.6	2.4	2.4
Electron energy scale	<1.0	4.1	<1.0	6.1
Electron energy resolution	<1.0	<1.0	<1.0	<1.0
$W+jets$ & Multi-jet	N/A	10	N/A	129
Total	10	18	11	132

Bumphunter Search Results

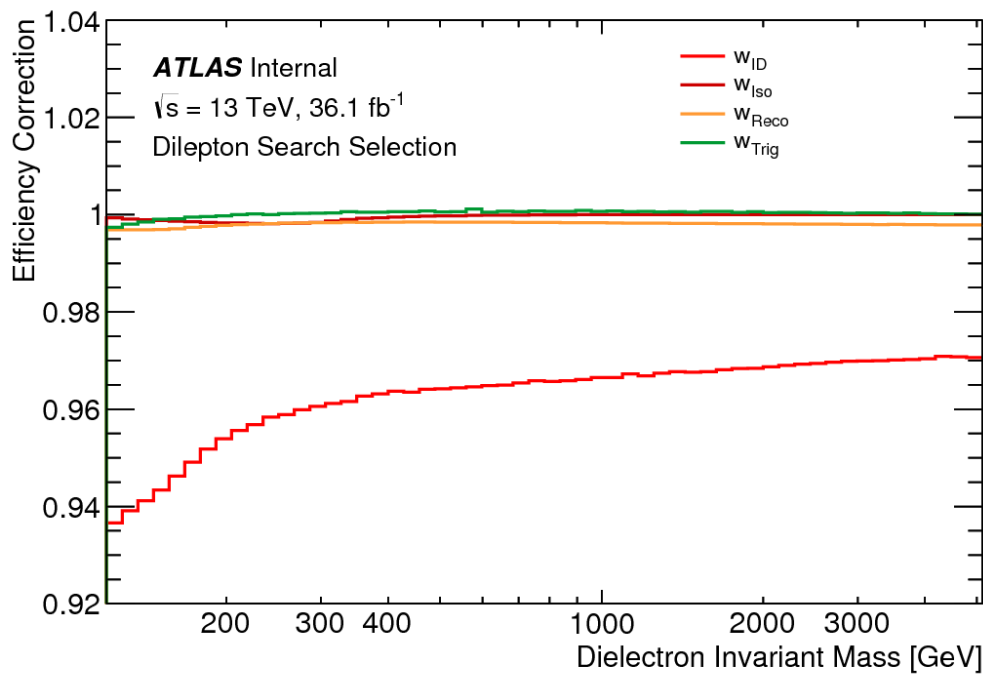
- Complimentary model independent approach with BumpHunter
 - Scans invariant mass windows for largest significance excess



- Global significance computed by throwing background only PEs
 - Electron channel: $p_{\text{global}} = 0.71$ (-0.56σ)
 - Muon channel: $p_{\text{global}} = 0.95$ (-1.61σ)

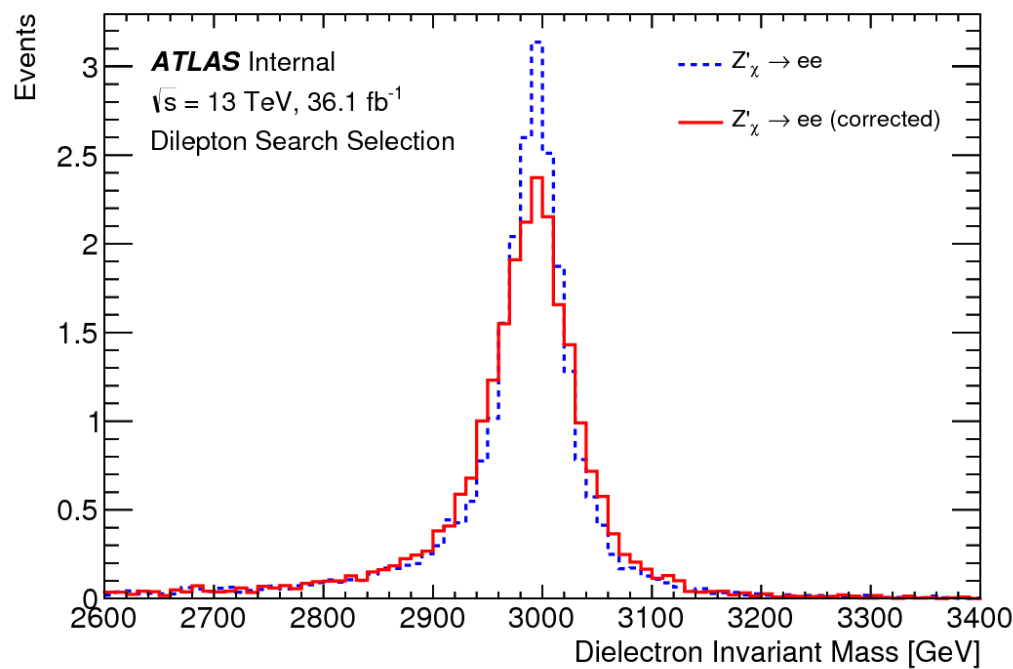
Background Modeling

- Need to correct simulation to obtain best possible agreement between data and MC
- Apply efficiency scale factor corrections



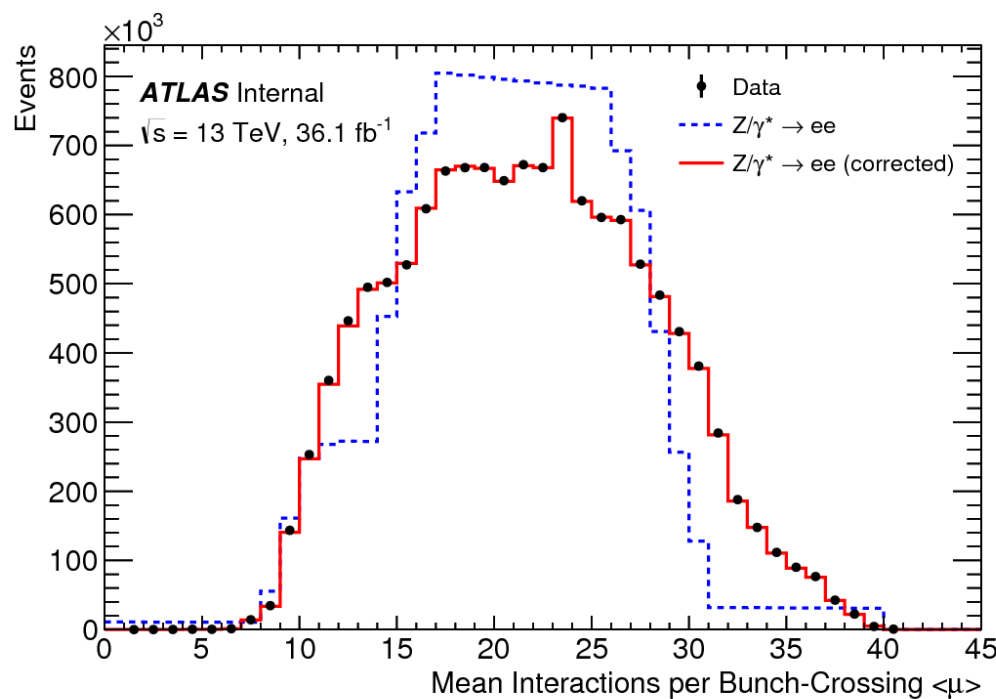
Background Modeling

- Need to correct simulation to obtain best possible agreement between data and MC
- Perform energy resolution smearing & energy scale correction



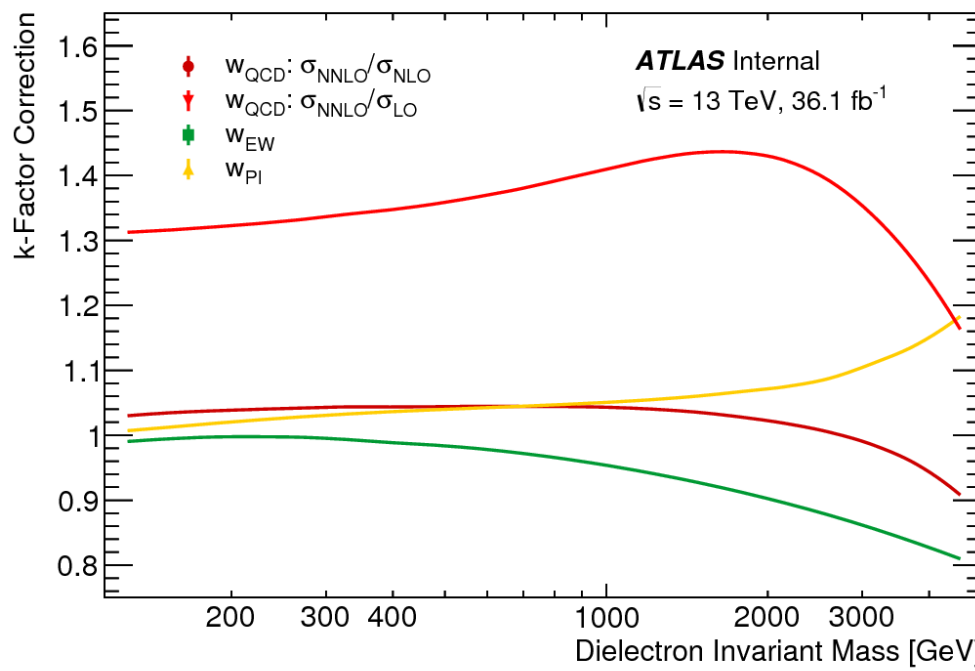
Background Modeling

- Need to correct simulation to obtain best possible agreement between data and MC
- Perform Pileup Reweighting



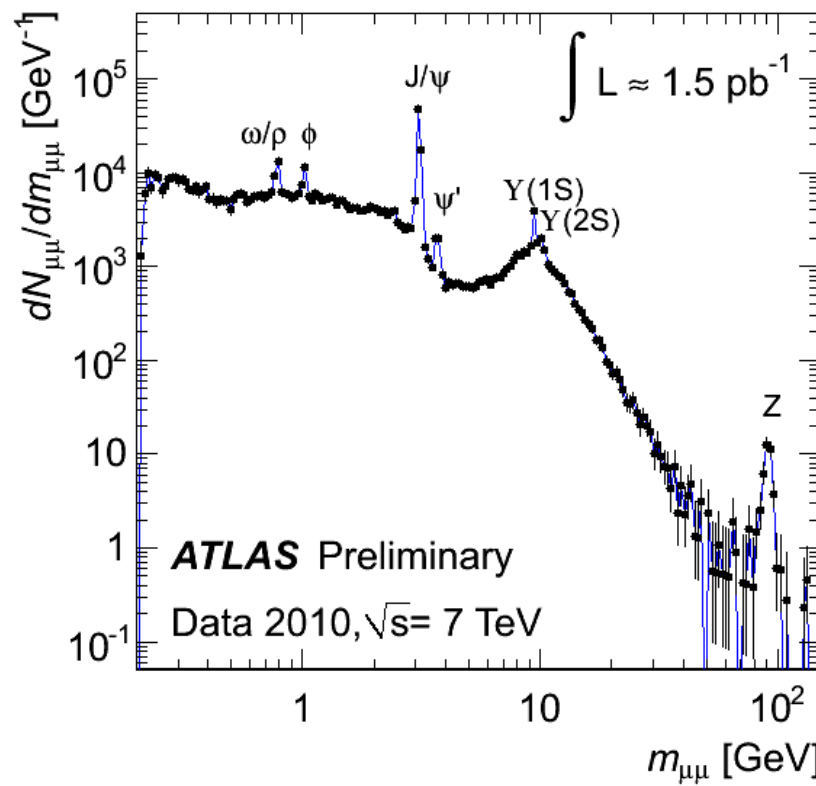
Background Modeling

- Need to correct simulation to obtain best possible agreement between data and MC
- Apply higher-order k-factor corrections



Past Resonances

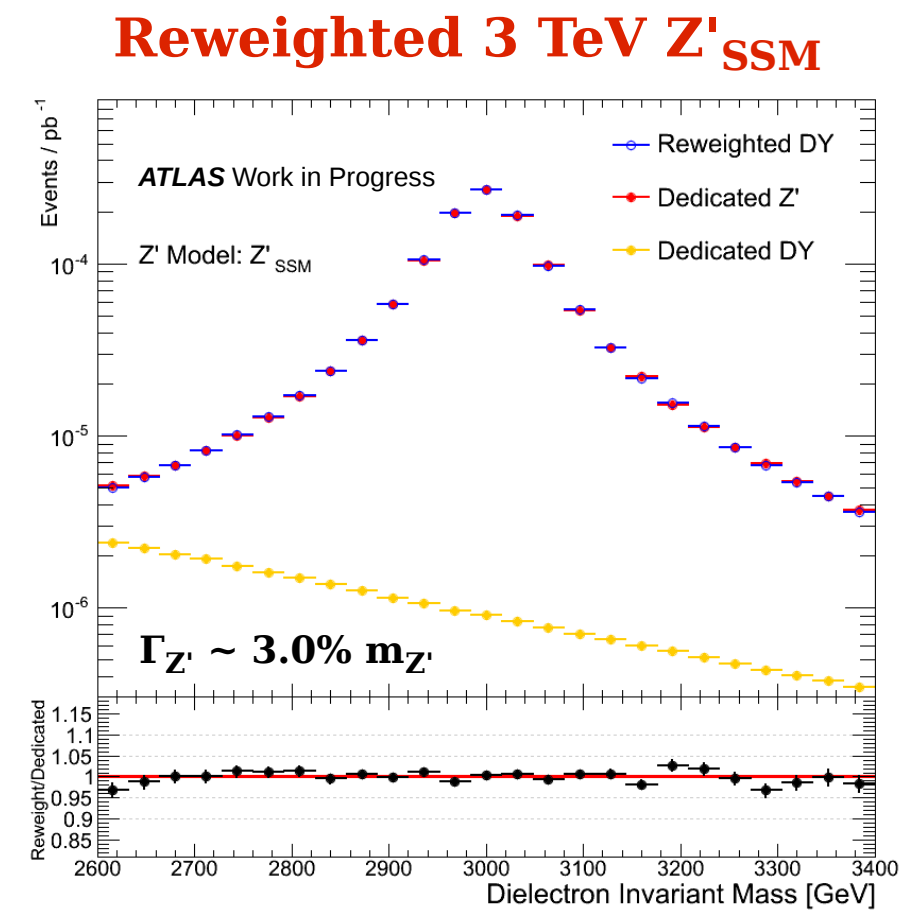
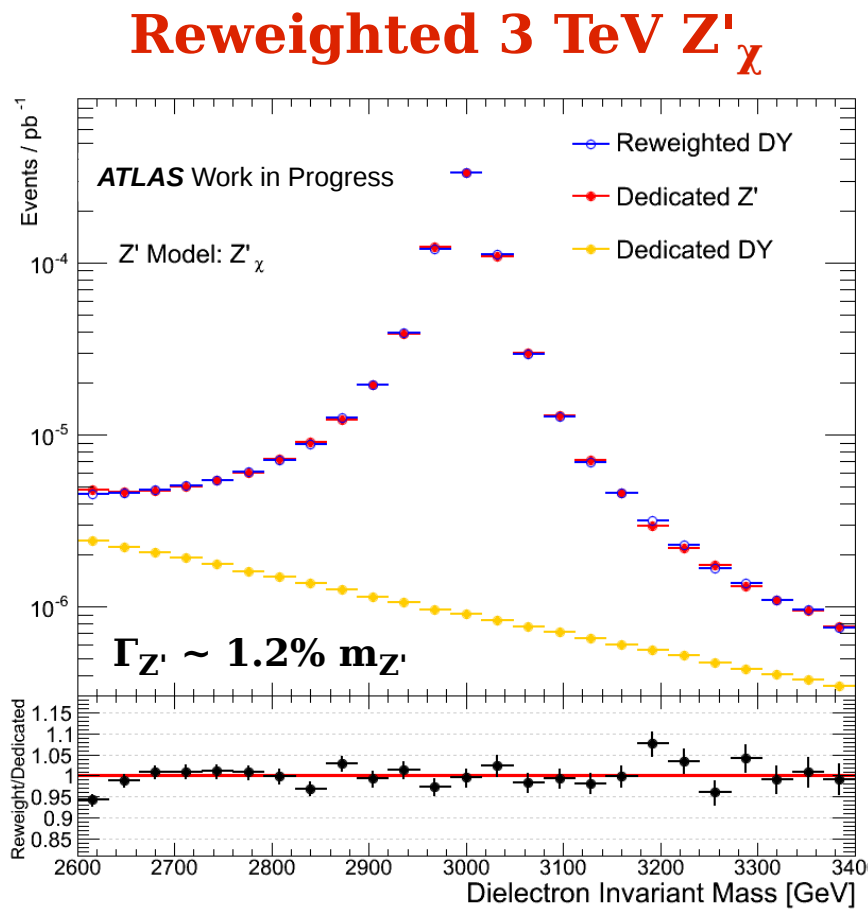
- Historically, dilepton final state is excellent place to search for new physics
- Discovery of c-quark, b-quark, Z boson



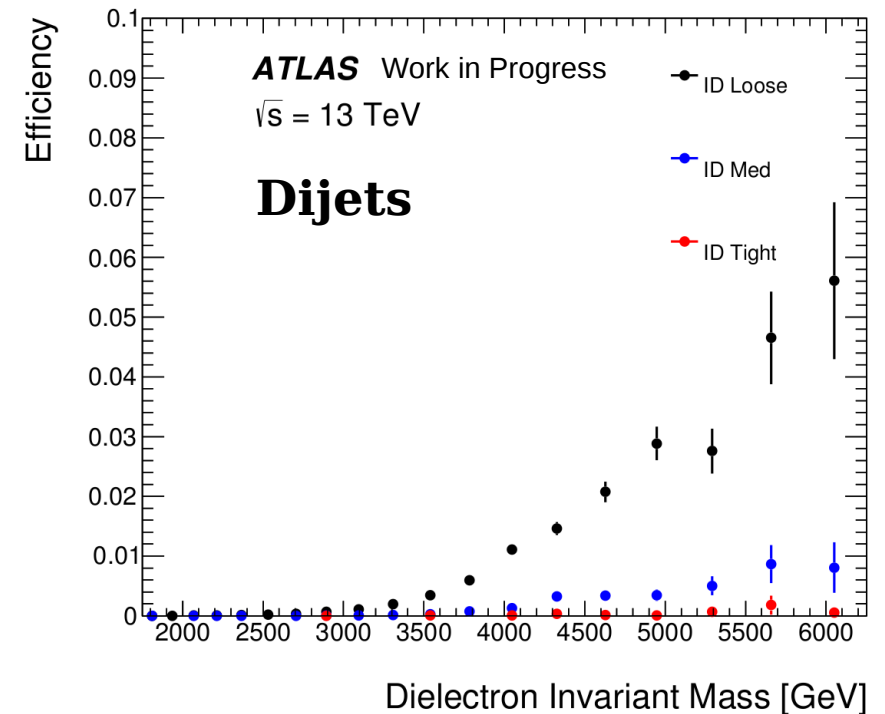
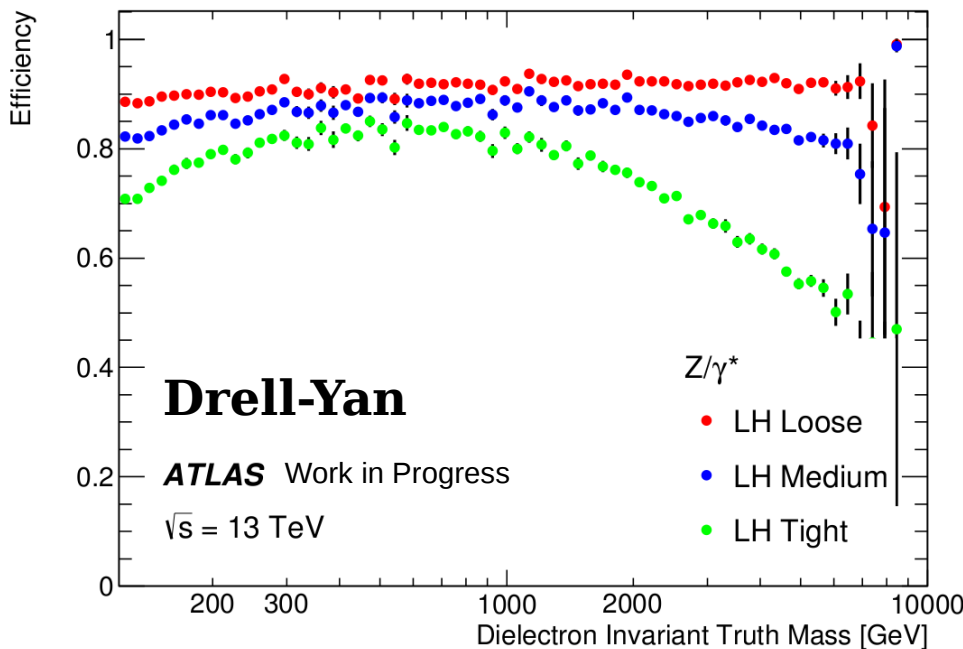
- New resonances address big questions (e.g. unification, new forces, dark matter, etc.)

Signal Samples

- Signal Template Reweighting
 - Drell-Yan event reweighted to Z' event at matrix element level
 - Include effect of DY/ Z' Interference
 - Reweight to multiple models and mass points for search/limit setting



Performance of Electron ID



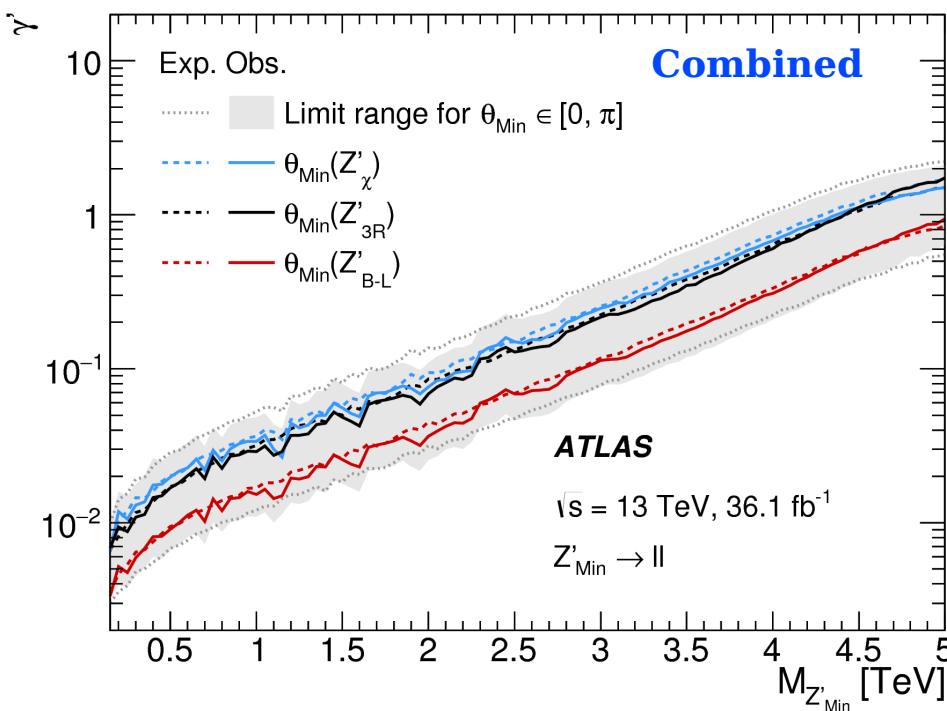
- Electron ID allows real high E_T electrons to be distinguished from mis-reconstructed jets
- Dielectron analysis optimized as a high-mass search
 - Find balance between signal acceptance and background rejection → use “Medium” electron ID working point

Exclusion Limits on Minimal Model

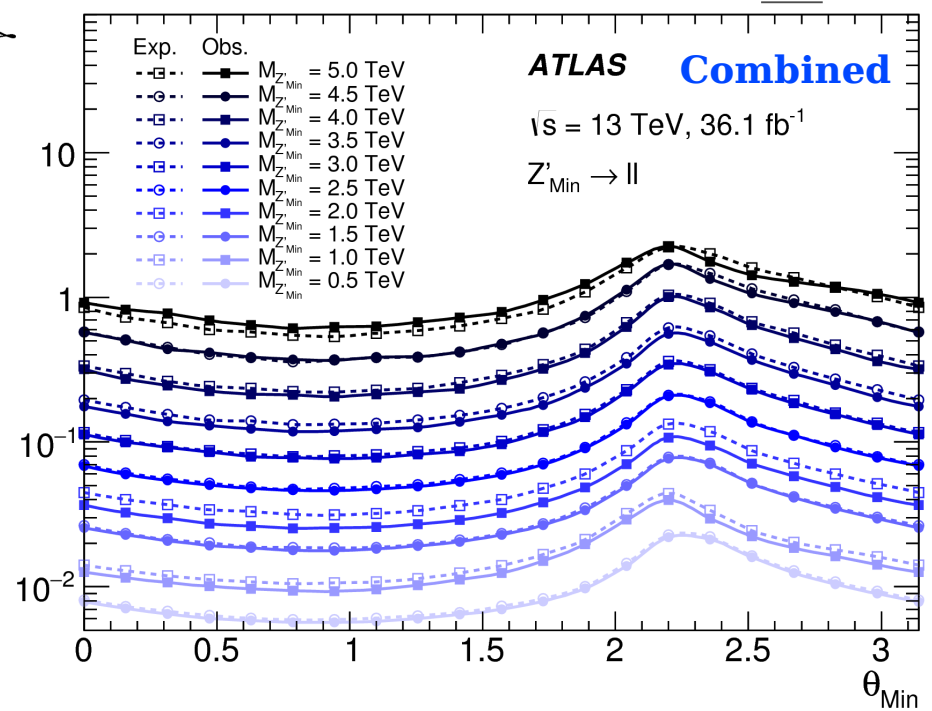
- Z' width and cross-section set by γ' , θ_{Min}
- Set limit on γ' as function of **1) Mass**, **2) θ_{Min}**
- Full SM+ Z' interference and finite Z' width included when reweighting

Model	γ'	$\tan \theta_{\text{Min}}$	Lower limits on $M_{Z'_{\text{Min}}}$ [TeV]					
			ee		$\mu\mu$		$\ell\ell$	
			Obs	Exp	Obs	Exp	Obs	Exp
Z'_X	$\sqrt{\frac{41}{24}} \sin \theta_{\text{Min}}$	$-\frac{4}{5}$	3.7	3.7	3.4	3.3	3.9	3.8
Z'_{3R}	$\sqrt{\frac{5}{8}} \sin \theta_{\text{Min}}$	-2	4.0	3.9	3.6	3.6	4.1	4.1
Z'_{B-L}	$\sqrt{\frac{25}{12}} \sin \theta_{\text{Min}}$	0	4.0	4.0	3.6	3.6	4.2	4.1

1) Limits as function of Mass

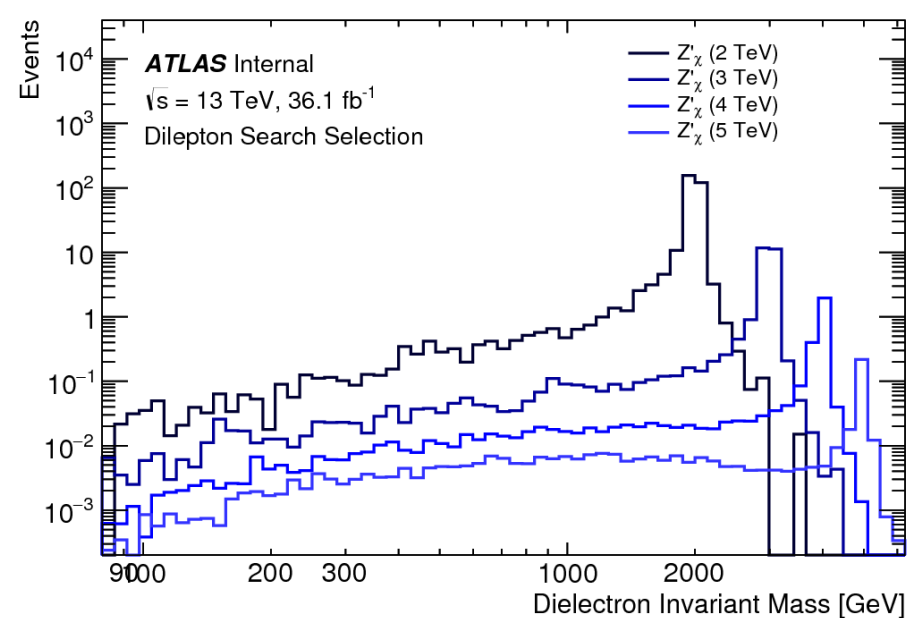
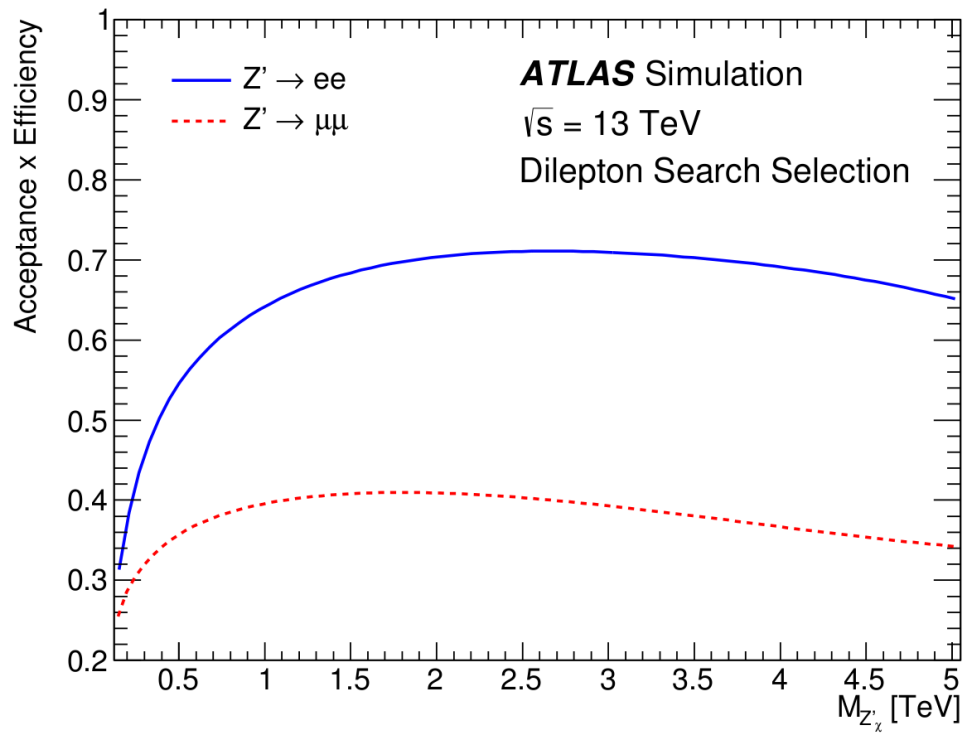


2) Limits as function of θ_{Min}



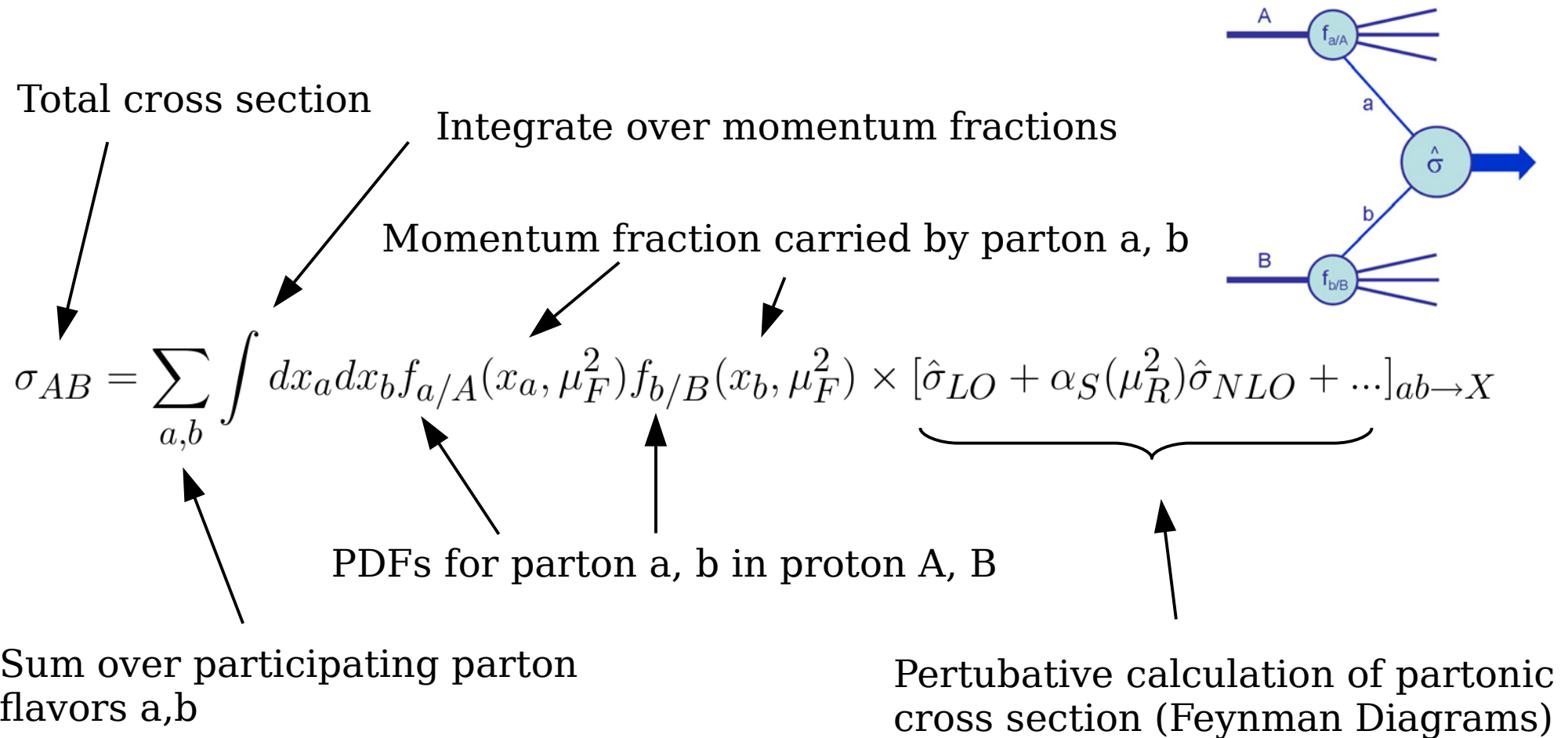
Signal Efficiency

→ Mass of Z' unknown a-priori, use event selection to assess signal efficiency as function of mass



→ A 3 TeV pole mass Z' boson has a 71% signal efficiency

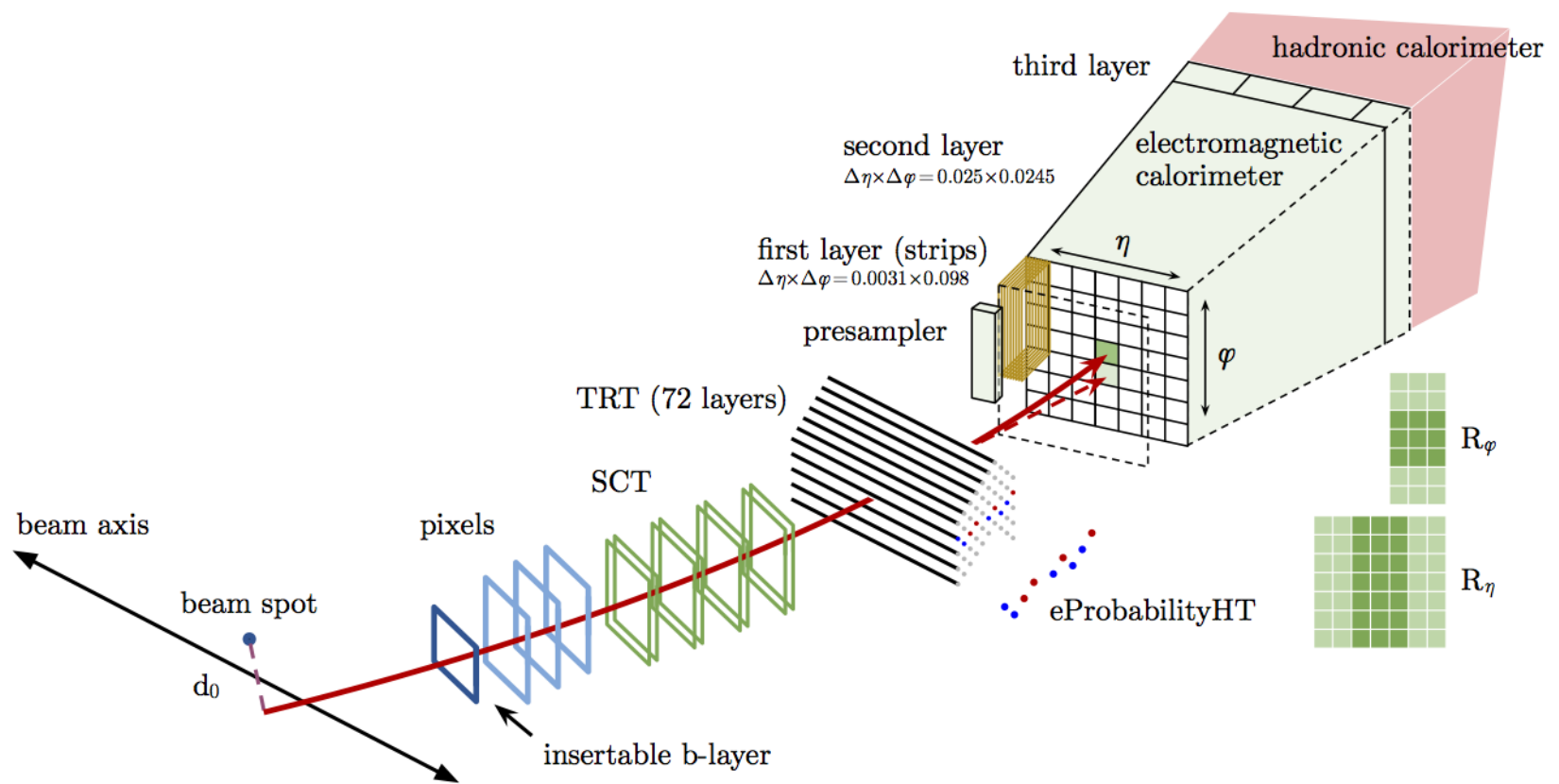
Parton Distribution Functions at the LHC



- Convolute fixed order partonic cross section with PDFs to estimate the total cross section at the LHC
- Uncertainties in PDFs are propagated to the estimate of the total cross section

Electron Reconstruction

- Electron candidate reconstructed from energy deposit in EM calorimeter matched to inner detector track
- Successful reconstructed results in electron four-vector



Dilepton Likelihood Function

$$\mathcal{L}(\mu, \boldsymbol{\theta}) = \prod_{k=1}^{N_{\text{bins}}} \frac{\lambda_k(\mu, \boldsymbol{\theta}) e^{-\lambda_k(\mu, \boldsymbol{\theta})}}{n_k!} \prod_{i=1}^{N_{\text{sys}}} \mathcal{N}(\theta_i, 0, 1)$$

$$\lambda_k(\mu, \boldsymbol{\theta}) = \mu s_k(\boldsymbol{\theta}) + b_k(\boldsymbol{\theta})$$

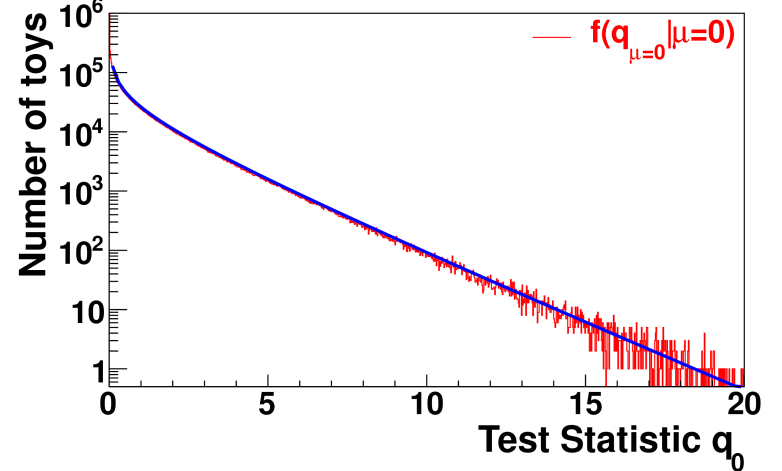


Signal expectation, Standard Model expectation in
dilepton mass bin k

Likelihood-Ratio Test

→ Construct Test Statistic q_0 :

$$q_0 = \begin{cases} 0, & \text{for } \hat{\mu} < 0 \\ -2 \ln \left[\frac{\mathcal{L}(0, \hat{\theta}_0)}{\mathcal{L}(\hat{\mu}, \hat{\theta})} \right], & \text{for } \hat{\mu} \geq 0 \end{cases}$$



→ Extract local p-value from test statistic sampling distribution:

$$p_0 = p(q_0 \geq q_0^{obs} | H_0) = \int_{q_0^{obs}}^{\infty} f(q_0 | 0) dq_0$$

→ Compare to global p-value:

$$p_{\text{global}} = p(z_0 \geq z_0^{obs} | H_0) = \int_{z_0^{obs}}^{\infty} n(z_0 | 0) dz_0$$

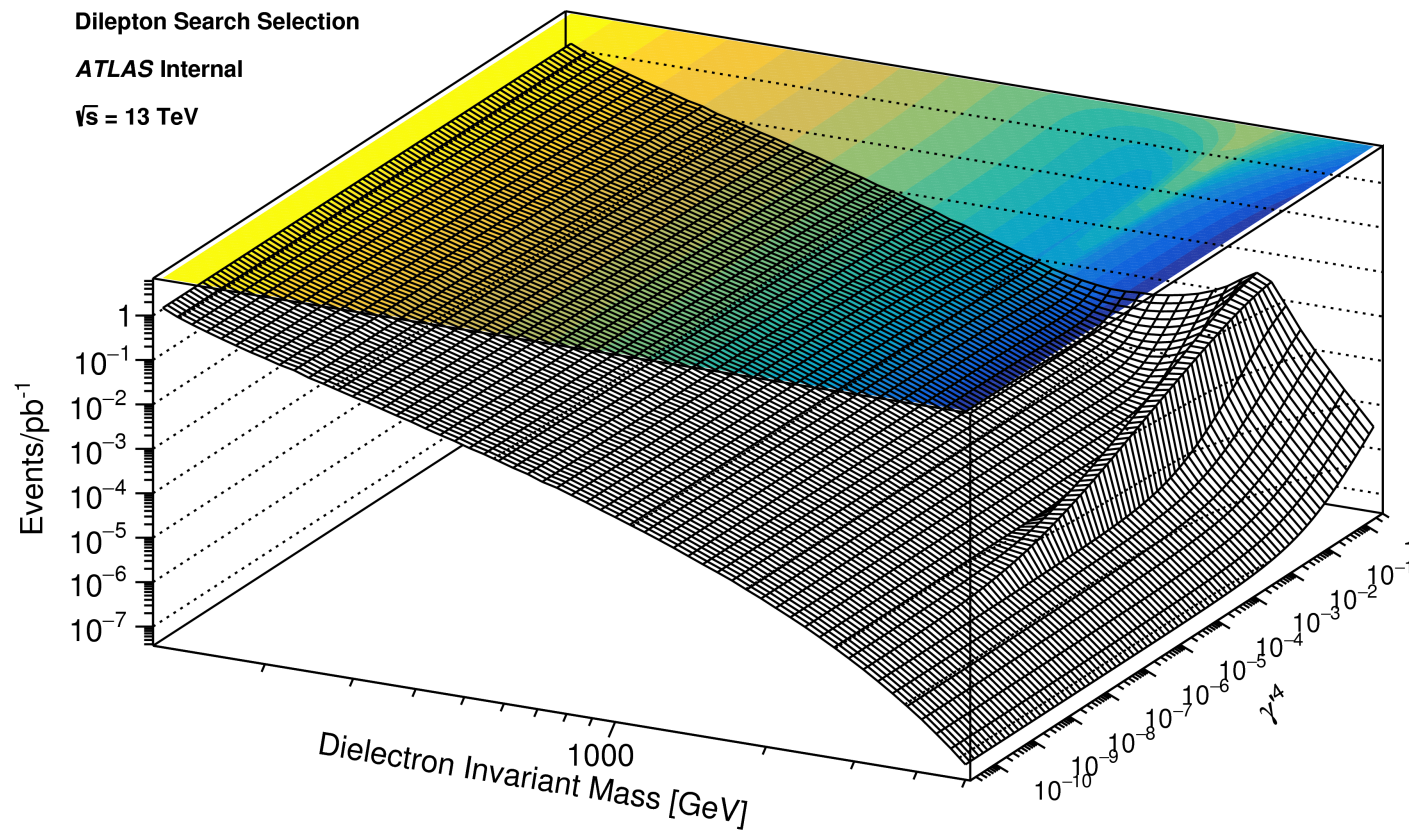
Addition of Muon Channel

→ In order to calculate combined limits, extend the nominal likelihood function:

$$\mathcal{L}(\mathbf{n}|\sigma B, \boldsymbol{\theta}) = \prod_{l=1}^{N_{\text{channel}}} \prod_{k=1}^{N_{\text{bins}}} \frac{\lambda_{lk}(\sigma B, \boldsymbol{\theta}) e^{-\lambda_{lk}(\mu, \boldsymbol{\theta})}}{n_{lk}!} \prod_{i=1}^{N_{\text{sys}}} \mathcal{N}(\theta_i, 0, 1)$$

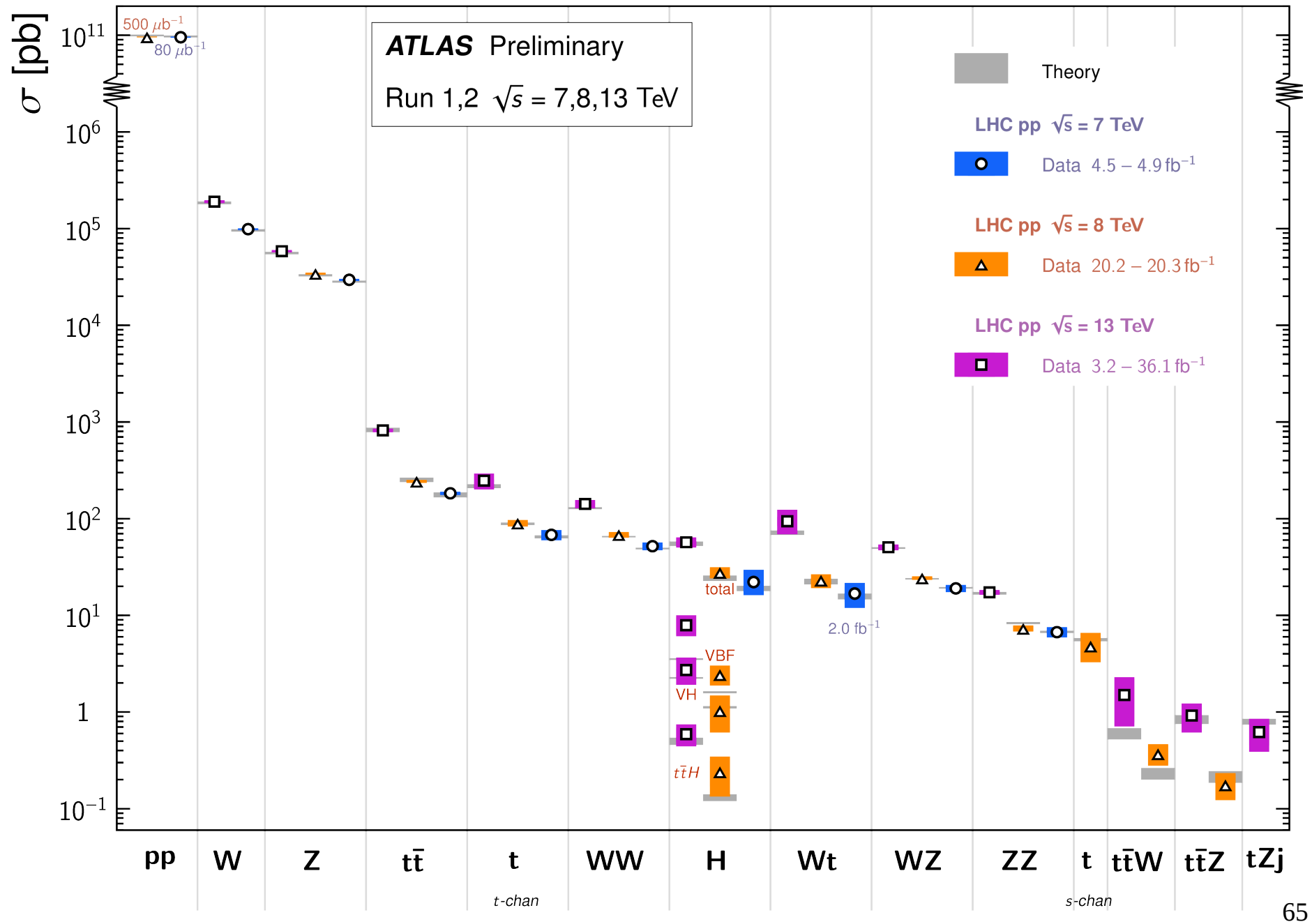
Construction of Minimal Model Templates

→ Two dimensional templates produced with signal reweighting

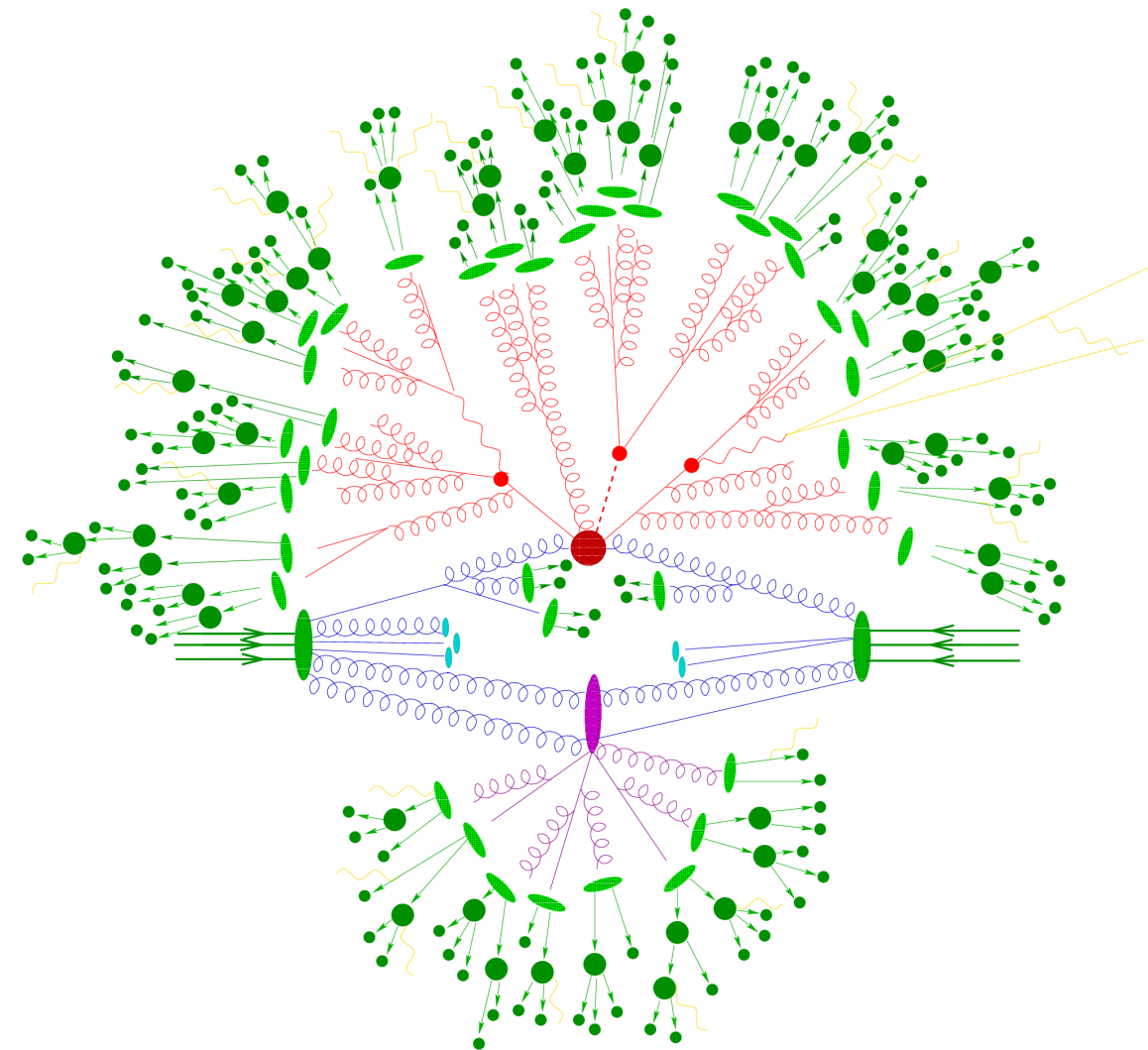


Standard Model Total Production Cross Section Measurements

Status: March 2018

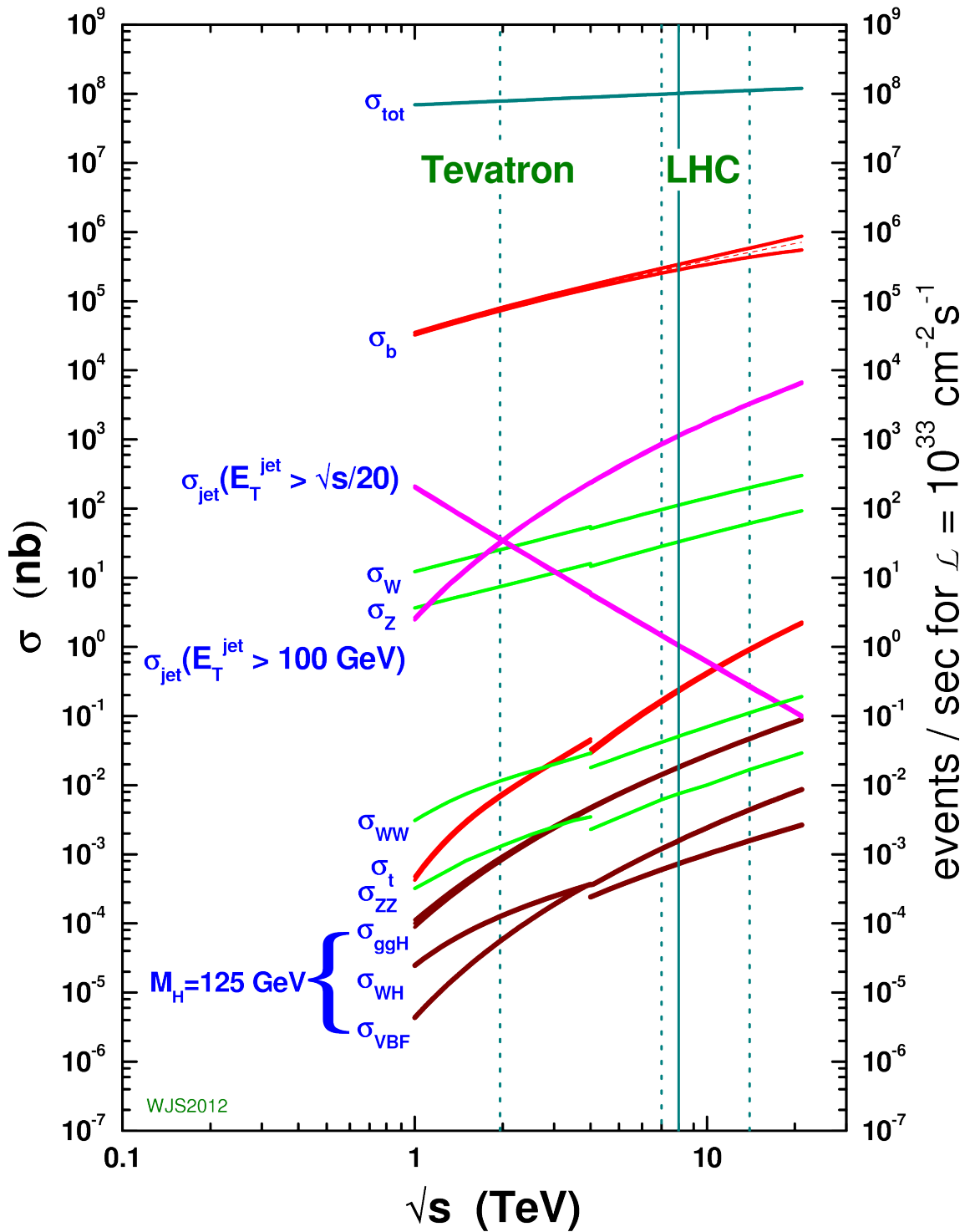


Hadronic Collisions at the LHC



- dark red blob, hard process
- red lines, final state radiation
- light blue lines, beam remnants
- dark blue lines, initial state radiation
- purple blob secondary hard
- purple lines, final state radiation
- light green blobs, hadronization
- dark green blobs, hadronic decays
- yellow lines, EM radiation

proton - (anti)proton cross sections



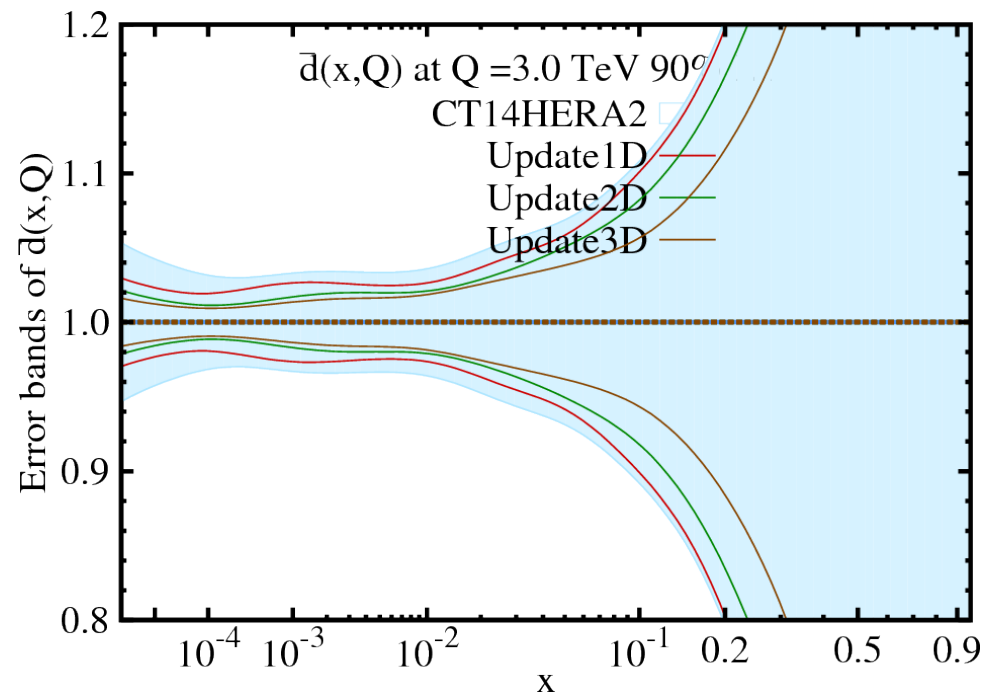
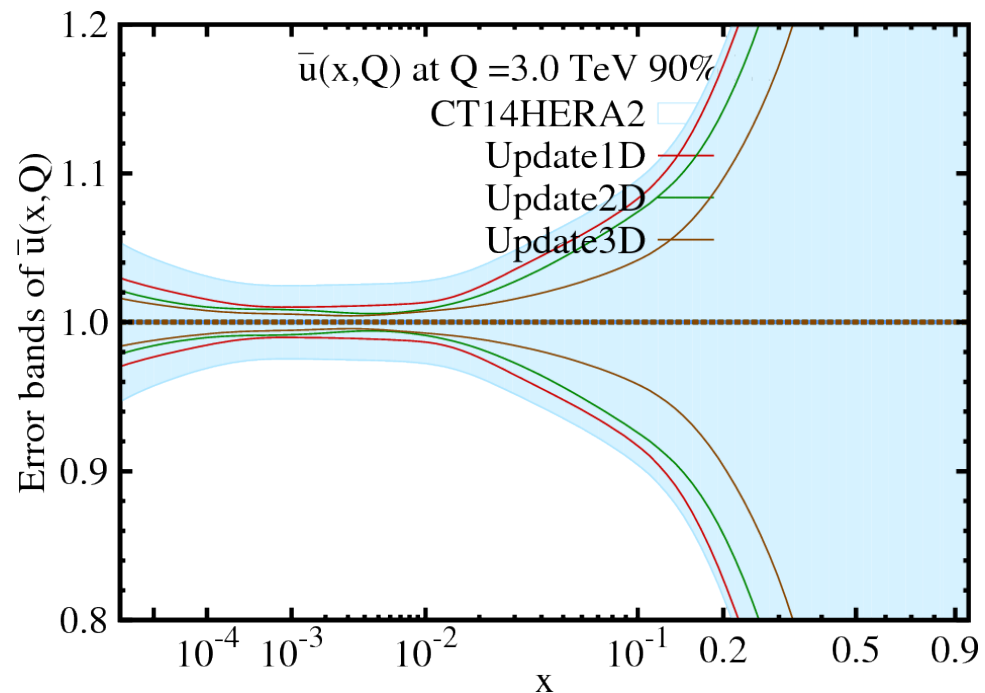
Reduction in PDF Uncertainty

→ Values obtained from the 3000/fb PDF update

x	$u_v(x)$		$d_v(x)$		$\bar{u}(x)$		$\bar{d}(x)$	
	δ_{pre} [%]	δ_{post} [%]						
0.1	3.4	0.7	5.8	1.5	9.8	2.2	11	3.8
0.3	2.6	0.9	7.5	3.6	30	8.3	32	11
0.5	4.8	2.6	16	11	71	20	69	20
0.7	12	7.0	45	30	280	77	250	67

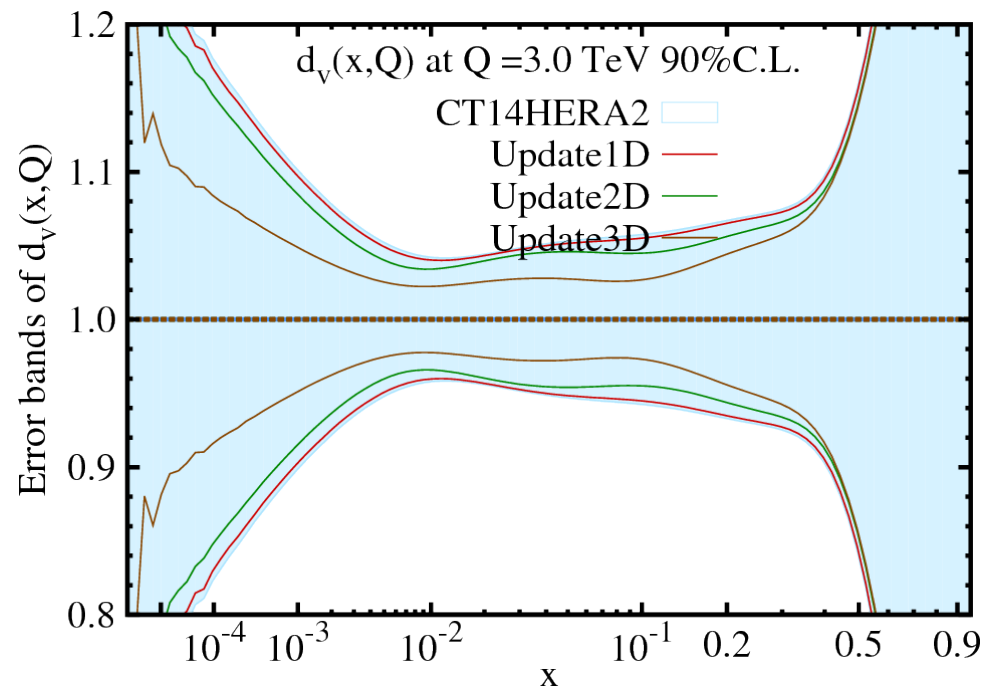
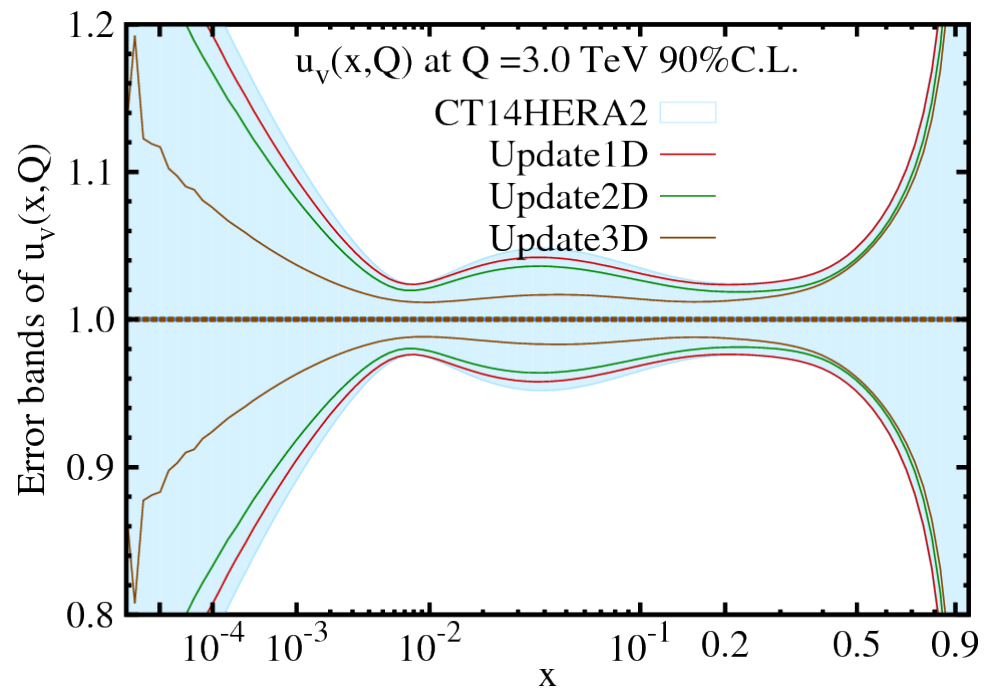
Update Impact on Valence PDFs

→ 300/fb PDF Update



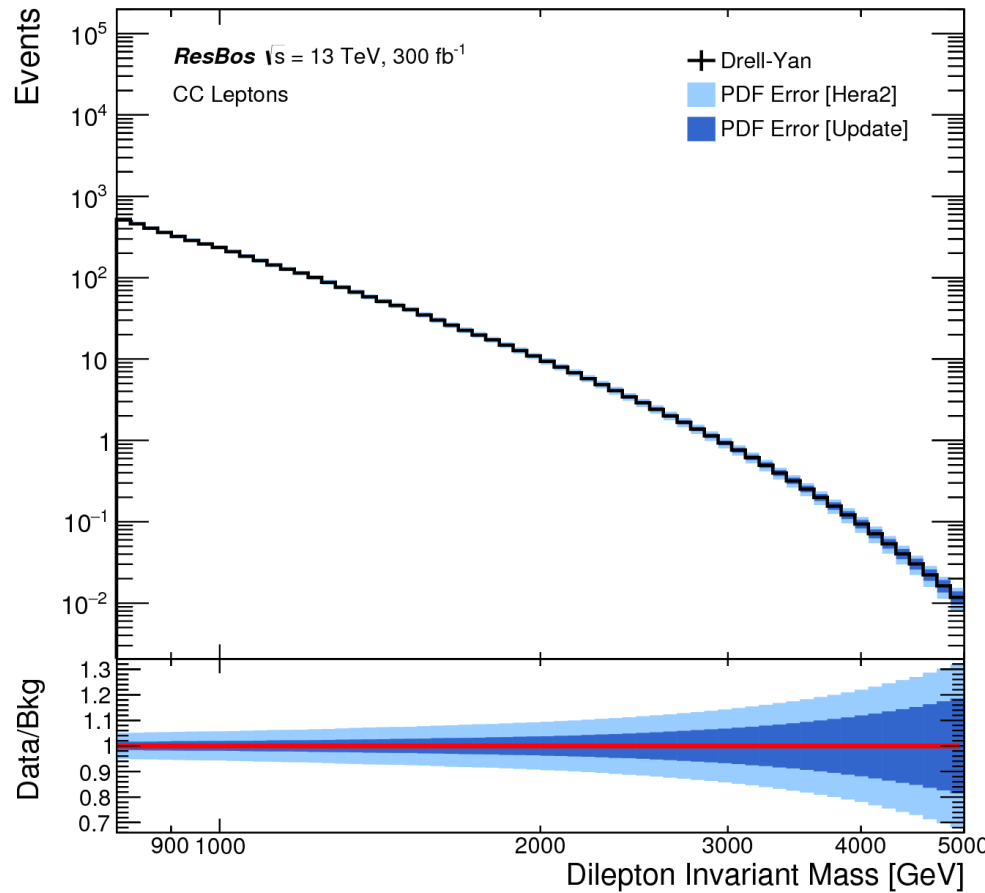
Update Impact on Sea PDFs

→ 300/fb PDF Update



Update Impact on high-mass Drell-Yan

→ 300/fb PDF Update



- At $m_{ll} = 5 \text{ TeV}$, PDF uncertainty reduced from 32% to 19%
- At $m_{ll} = 3 \text{ TeV}$, PDF uncertainty reduced from 15% to 7.1%
- PDF uncertainties reduced to comparable level of current dilepton experimental uncertainties

ePump Templates constructed triple-differentially

→ In slices of m_{ll} , $|y_{ll}|$, $\cos\theta^*$, 1296 bins total, pseudo-data generated at 3000/fb

